

Review Article

Open Access



# A review: flexible devices for nerve stimulation

Ze-Qing Liu<sup>1,#</sup>, Xiang-Yang Yu<sup>1,#</sup>, Jing Huang<sup>1,#</sup>, Xin-Yi Wu<sup>1,#</sup>, Zi-Yu Wang<sup>2,\*</sup>, Ben-Peng Zhu<sup>1,3,\*</sup>

<sup>1</sup>School of Integrated Circuits, Wuhan National Laboratory for Optoelectronics, Huazhong University of Science and Technology, Wuhan 430074, Hubei, China.

<sup>2</sup>The Institute of Technological Sciences, Wuhan University, Wuhan 430072, Hubei, China.

<sup>3</sup>State Key Laboratory of Transducer Technology, Chinese Academy of Sciences, Shanghai 200050, China.

#Authors contributed equally.

\*Correspondence to: Prof. Ben-Peng Zhu, School of Integrated Circuits, Huazhong University of Science and Technology, No. 1037 Luoyu Road, Wuhan 430074, Hubei, China. E-mail: benpengzhu@hust.edu.cn; Prof. Zi-Yu Wang, The Institute of Technological Sciences, Wuhan University, No. 299 Bayi Road, Wuhan 430072, Hubei, China. E-mail: zywang@whu.edu.cn

**How to cite this article:** Liu ZQ, Yu XY, Huang J, Wu XY, Wang ZY, Zhu BP. A review: flexible devices for nerve stimulation. *Soft Sci* 2024;4:4. <https://dx.doi.org/10.20517/ss.2023.36>

**Received:** 16 Aug 2023 **First Decision:** 7 Oct 2023 **Revised:** 30 Oct 2023 **Accepted:** 23 Nov 2023 **Published:** 10 Jan 2024

**Academic Editor:** Zhifeng Ren **Copy Editor:** Dong-Li Li **Production Editor:** Dong-Li Li

## Abstract

Nerve stimulation technology utilizing electricity, magnetism, light, and ultrasound has found extensive applications in biotechnology and medical fields. Neurostimulation devices serve as the crucial interface between biological tissue and the external environment, posing a bottleneck in the advancement of neurostimulation technology. Ensuring safety and stability is essential for their future applications. Traditional rigid devices often elicit significant immune responses due to the mechanical mismatch between their materials and biological tissues. Consequently, there is a growing demand for flexible nerve stimulation devices that offer enhanced treatment efficacy while minimizing irritation to the human body. This review provides a comprehensive summary of the historical development and recent advancements in flexible devices utilizing four neurostimulation techniques: electrical stimulation, magnetic stimulation, optic stimulation, and ultrasonic stimulation. It highlights their potential for high biocompatibility, low power consumption, wireless operation, and superior stability. The aim is to offer valuable insights and guidance for the future development and application of flexible neurostimulation devices.

**Keywords:** Nerve stimulation, flexible devices, electrical stimulation, magnetic stimulation, optic stimulation, ultrasonic stimulation



© The Author(s) 2024. **Open Access** This article is licensed under a Creative Commons Attribution 4.0 International License (<https://creativecommons.org/licenses/by/4.0/>), which permits unrestricted use, sharing, adaptation, distribution and reproduction in any medium or format, for any purpose, even commercially, as long as you give appropriate credit to the original author(s) and the source, provide a link to the Creative Commons license, and indicate if changes were made.



## INTRODUCTION

Certain chronic neurological disorders, including epilepsy, Parkinson's disease, and Alzheimer's disease, can lead to various dysfunctions in affected individuals. The application of neurostimulation has shown promise in alleviating and improving impairments related to movement and cognition, ultimately enhancing the overall quality of life. The research on electrical-based nerve stimulation for treating neurological diseases in humans has a long-standing history dating back to the previous century and has had a profound clinical impact. Under normal physiological conditions, nerve cells transmit nerve impulses through action potentials to carry out their functions. In pathological conditions, neurostimulation treatments modify or achieve brain function by delivering electrical signals to neurons. For example, deep brain stimulation (DBS) involves the implantation of electrodes into specific brain regions, allowing the stimulation current generated by the pulse generator to flow along the electrodes and produce therapeutic effects.

Neurostimulation devices are utilized to establish a connection between the nervous system and the external environment, playing a vital role in neural recording and stimulation. The majority of early neural interfaces were rigid, such as Galvani bimetal arch wire, Fritsch lead wire, and Hubel microwire<sup>[1]</sup>. The implantation of these rigid electrodes in animals can lead to tissue damage, foreign body rejection, and device performance degradation. Innovative advancements in materials and microfabrication technology have paved the way for the fabrication of stretchable, bendable, and highly biocompatible flexible neurostimulation devices, providing a promising alternative. Extensive research is dedicated to the design of advanced device structures and the development of flexible materials. Materials with excellent biocompatibility [e.g., polyimide, polydimethylsiloxane, carbon nanotubes (CNT), hydrogel, parylene, and silk fibroin]<sup>[2-4]</sup> can be utilized as substrates or coating materials to prepare implantable or wearable flexible neurostimulation devices. This approach can achieve effective interface matching between electronic devices and biological tissues, minimize tissue damage, and enhance the safety of biological applications, all while maintaining the desired nerve stimulation effect. Researchers primarily employ flexible materials to replace rigid components in existing devices, create composite materials by combining flexible and functional components, utilize flexible materials as coatings for functional components such as conductive materials, and explore the development of nanomaterials with stimulating properties, among other approaches. Furthermore, traditional direct electrical stimulation (ES) using implanted electrodes faces challenges in achieving both safe and non-invasive nerve stimulation effects with high spatial precision, resulting in certain limitations<sup>[5]</sup>. As a result, researchers are increasingly focused on the investigation of flexible devices that utilize energy and information transmission mediums such as magnetism, light, and ultrasound. For instance, one notable example is the use of low-energy infrared light for non-invasive stimulation<sup>[6]</sup> and the application of transcranial focused ultrasound to non-invasively modulate human brain function<sup>[7]</sup>. These flexible devices offer the advantages of compact size and wireless operation, with the potential to achieve long-term stability and high-quality neuromodulation and treatment in complex environments.

This review aims to summarize the recent advancements in flexible neurostimulation devices. These devices are categorized into four groups based on different stimulation methods: ES, magnetic stimulation (MS), optic stimulation, and ultrasound stimulation [Figure 1]. More importantly, this review analyzes how flexible neurostimulation devices can meet specific size, safety, and ductility requirements through principle design, material selection, and structural design under various neurostimulation methods. Additionally, the challenges of flexible electronic devices for neurostimulation are discussed, highlighting that high biocompatibility, wireless functionality, long-term stability, and closed-loop stimulation are the key obstacles and future development trends for flexible neurostimulation devices.



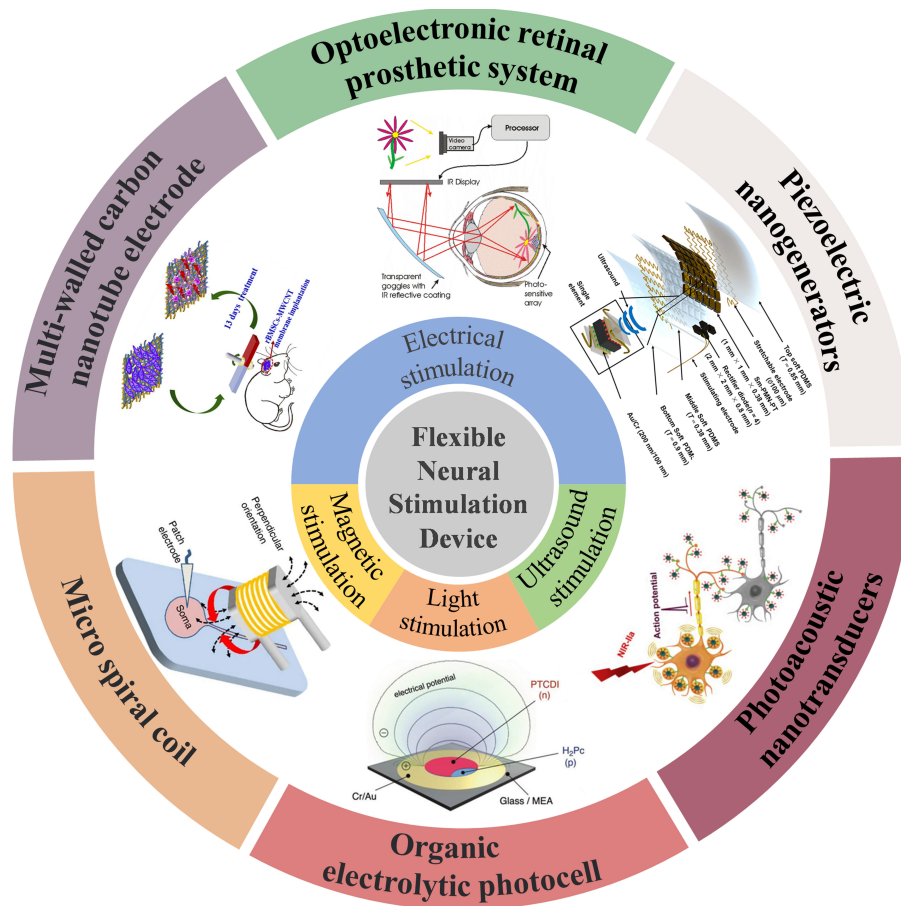


**Figure 1.** Flexible devices for electrical, magnetic, optical, and ultrasonic stimulation. Figure “Multi-walled carbon nanotube electrode”<sup>[8]</sup>, reprinted with permission. Copyright 2022, Elsevier; Figure “Optoelectronic retinal prosthetic system”<sup>[9]</sup>, reprinted with permission. Copyright 2005, IOP Publishing; Figure “Piezoelectric nanogenerators”<sup>[10]</sup>, reprinted with permission. Copyright 2021, AAAS; Figure “Micro spiral coil”<sup>[11]</sup>, reprinted with permission. Copyright 2012, Springer Nature; Figure “Organic electrolytic photocell”<sup>[12]</sup>, reprinted with permission. Copyright 2018, John Wiley and Sons; Figure “Photoacoustic nanotransducers”<sup>[13]</sup>, reprinted with permission. Copyright 2020, Elsevier.

## ELECTRICAL STIMULATION

ES induces functional responses by modulating the membranes of excitable cells and altering the potential and activity of nerves and other tissues<sup>[14]</sup>. As early as 46 AD, electric stingrays were utilized for treating headaches and other ailments<sup>[15]</sup>. The medical application of ES became prevalent in the 19th century, particularly after the discovery in the 1870s that applying different levels of electricity to dogs produced varying intensities of response, ranging from localized limb movements to full-body reactions<sup>[16]</sup>. These early experiments laid the foundation for the development of numerous devices for electrical nerve stimulation. With the advancements in flexible electronics, devices used for electrical nerve stimulation have transitioned from rigid to flexible designs.

### Direct electrical stimulation

Since the 1940s, Electroconvulsive therapy (ECT) has been utilized as an effective method for treating severe mood or pain disorders<sup>[17]</sup>. In 1987, Benabid *et al.* employed DBS to treat Parkinson’s disease<sup>[18]</sup>. DBS is a technology that implants electrodes into the brain to deliver electric current, stimulating different parts of the brain. It has shown promising clinical performance; However, due to the use of rigid electrodes, various chronic neurological complications, intracranial hemorrhage, or infections may occur<sup>[19]</sup>. The elastic

modulus of rat brain tissue is about 0.03 to 1.75 kPa<sup>[20]</sup>, while that of silicon, tungsten, and other metals or inorganic semiconductor materials typically exceeds 100 GPa<sup>[21]</sup>. This mismatch in mechanical properties can lead to neuron death or device aging and failure during implantation or movement. Therefore, the usage of flexible devices is becoming a current development trend.

To effectively mitigate the inflammatory response elicited by tissues, flexible devices for direct electrical nerve stimulation employ flexible base materials, electrode materials, or coating materials. This approach effectively addresses the challenge of mismatched mechanical and electrical properties at the interface between neural electrodes and biological tissues, thereby ensuring optimal stimulation and stability.

#### *Flexible base material*

Polymer materials, such as flexible polyimide substrates, offer superior biocompatibility compared to hard materials, such as silicon and platinum, when used as substrate materials for nerve electrodes. Lai *et al.* designed an implantable micromachined neural probe with a multi-channel electrode array<sup>[22]</sup>. The flexible polyimide-based microelectrode array, as depicted in [Figure 2A](#), comprises a long axis (14.9 mm in length) and 16 electrodes (5  $\mu\text{m}$  thick, 16  $\mu\text{m}$  in diameter). These microelectrode lineups are capable of flexing during implantation. The obtained somatosensory evoked potentials (SSEPs) through thalamic stimulation and the *in vivo* measurements of electrode-electrolyte interface impedance remain stable for a duration of up to 50 days. The reliability of these probes in DBS applications in animals has been verified, making them suitable for long-term stimulation. Wurth *et al.* investigated the long-term stability of SELINE polyimide-based intra-neural implants<sup>[23]</sup>. The implants in 28 mice exhibited normal function six months after insertion, thus demonstrating the potential of polyimide-based neural implants for long-term clinical applications. Fujie *et al.* developed freestanding ultrathin polymeric films, referred to as “nanomembranes”, using polystyrene (PS)<sup>[24]</sup>. These nanomembranes can serve as powerful tools for the development of flexible biological devices and applications in regenerative medicine. However, when utilizing polymer materials to enhance flexibility, it becomes challenging to penetrate the nerve tissue. To ensure probe stiffness for withstanding insertion force and achieving accurate positioning, this challenge can be addressed by coating the probe with biodegradable materials. Xiang *et al.* developed an ultra-thin flexible polyimide neural probe, as shown in [Figure 2B](#), with an overall thickness of merely 10  $\mu\text{m}$ <sup>[25]</sup>. To prevent the stiffness from becoming too low to penetrate the nerve tissue due to thickness shrinkage, they coated it with maltose, a biodegradable and biocompatible material, to enhance stiffness. This polyimide-based probe type can mitigate issues arising from micro-motion between the probe and biological tissue, thereby facilitating long-term applications, reducing size, and minimizing glial growth.

#### *Flexible electrode material*

Flexible neural electrodes play a crucial role in establishing connections between biological tissues and external devices. Minev *et al.* designed and engineered neural interfaces called e-dura, which incorporate interconnects, electrodes, and chemotrodes<sup>[26]</sup>. These electrodes have undergone ES pulses and mechanical stretch cycles, demonstrating their electrochemical stability, mechanical robustness, and long-term functionality. Carbon materials, such as CNTs, exhibit high electrical conductivity, flexibility, and chemical stability<sup>[27]</sup>. They can reduce device size and provide advantages such as MRI compatibility. As shown in [Figure 2C](#), David-Pur *et al.* proposed a novel flexible neuronal microelectrode device that utilizes multi-walled carbon nanotubes (MWCNT) films embedded in flexible polymer support, enabling seamless CNT circuits on flexible substrates<sup>[28]</sup>. As shown in [Figure 2D](#), Vitale *et al.* insulated a single CNT fiber 31 with a 3  $\mu\text{m}$ -thick layer of PS copolymer, leaving only the tips exposed as electrically active sites<sup>[29]</sup>. These electrodes were used in DBS experiments for Parkinson’s disease in rats, confirming the precise implantation of flexible CNT fiber microelectrodes in deep brain structures and their ability to selectively

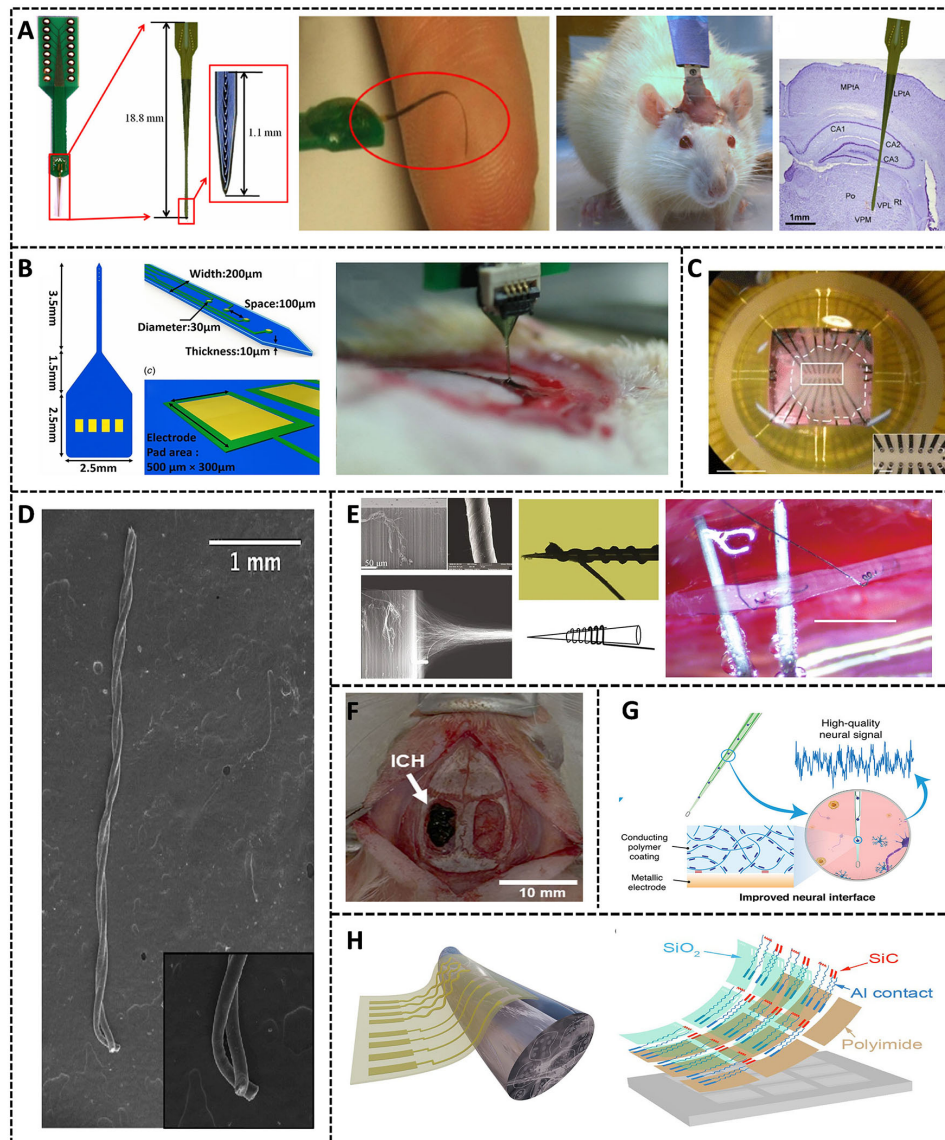


**Figure 2.** Flexible devices for direct electrical nerve stimulation. (A) Schematic diagram of the polyimide-based neural probe, showing the flexibility of the probe, which can still move freely after being implanted in the mouse brain region<sup>[22]</sup>. Reprinted with permission. Copyright 2012, IOP Publishing; (B) Schematic diagram of the ultra-thin flexible polyimide neural probe. After successfully penetrating, the brain maltose dissolves, and the rigid probe becomes a flexible neural probe<sup>[25]</sup>. Reprinted with permission. Copyright 2014, IOP Publishing; (C) Scanning electron microscope imaging of flexible CNT electrode array mounted on PCB holder<sup>[28]</sup>. Reprinted with permission. Copyright 2014, Springer Nature; (D) Dual-channel CNT fiber microelectrode<sup>[29]</sup>. Reprinted with permission. Copyright 2015, American Chemical Society; (E) CNT yarns with a diameter of 10  $\mu\text{m}$ , wound on tungsten for implantation in a nerve, and the distance between the two CNT yarns after implantation is about 2 mm<sup>[30]</sup>. Reprinted with permission. Copyright 2017, Springer Nature; (F) Photograph of the implantable ICH<sup>[34]</sup>. Reprinted with permission. Copyright 2023, Soft Science; (G) Schematic diagram of the metal electrode coated with the conductive polymer hydrogel (PEDOT:PSS), which can endow the electrode with superior biocompatibility and electrical and mechanical properties<sup>[35]</sup>. Reprinted with permission. Copyright 2023, Wiley-VCH GmbH; (H) Flexible SiC/SiO<sub>2</sub> bioelectronic system for stimulating the sciatic nerve<sup>[36]</sup>. Reprinted with permission. Copyright 2022, PANS. CNT: Carbon nanotubes; ICH: injectable conductive hydrogel; PCB: printed circuit board; PEDOT:PSS: poly(3,4-ethylenedioxythiophene)-poly(styrenesulfonate).

deliver the required stimulation charge for treatment. On this basis, McCallum *et al.* utilized CNT manufacturing technology to spin CNTs into yarns with a diameter of merely 10  $\mu\text{m}$ <sup>[30]</sup>. They then applied a thin parylene C layer (3.5  $\mu\text{m}$  thick) onto the CNTs. As depicted in [Figure 2E](#), when the yarn was wrapped

around tungsten microneedles and implanted into rats for 16 weeks, its electrical conductivity and flexibility increased tenfold, demonstrating the relative stability of the CNT yarn electrode within the nerve and confirming the feasibility of long-term stimulation. CNT-based electrodes are easy to fabricate and are resistant to bending. They effectively minimize brain damage and exhibit excellent interfacial electrochemical performance, making them ideal for biological brain stimulation applications. Furthermore, room-temperature liquid metals (LM) possess good fluidity and excellent electrical conductivity, making them suitable for long-term neurostimulation applications. For instance, Tang *et al.* developed fluid cuff electrodes that utilize gallium-based LM conductors to achieve long-term stimulation of peripheral nerves<sup>[31]</sup>.

#### *Flexible coating material*

Hydrogel materials possess excellent electrochemical properties and good stretchability, flexibility, adhesion, and biocompatibility<sup>[32]</sup>. They can adhere to both metal materials and biological tissues through mechanisms such as covalent bonds and classical absorption<sup>[33]</sup>. This property makes them ideal interface materials for connecting flexible electronic devices with biological tissues. Kim *et al.* developed an injectable purely conductive hydrogel (ICH) comprising tyramide-conjugated hyaluronic acid (HATYR) and poly(3,4-ethylenedioxythiophene)-poly(styrenesulfonate) (PEDOT:PSS). They also prepared ICH-based array device electrodes<sup>[34]</sup> [Figure 2F]. Animal experiments demonstrated the biocompatibility of ICH, enabling stable monitoring and highly sensitive recording of neural responses to visual stimulation. Zhang *et al.* designed robust conductive hydrogel coatings on conventional metal bioelectrodes<sup>[35]</sup> [Figure 2G]. The researchers implanted bioelectrodes coated with PEDOT:Poly (SS-4VP) into the bilateral dHPCs of freely moving mice and applied cyclic pulses for ES. The electrode's electrochemical properties remained nearly unchanged during the four-week testing period, confirming its suitability for long-term local ES. Nguyen *et al.* utilized broadband gap semiconductor nanofilms as biological interfaces<sup>[36]</sup> capable of sustaining electronic components for decades. The device, as depicted in Figure 2H, employs crystalline silicon carbide (SiC) nanomembranes as a faradic interface and silicon dioxide (SiO<sub>2</sub>) as an encapsulation layer. It exhibits excellent hydrolysis resistance and a high dielectric constant, making it suitable as a long-term stable biological barrier.

#### **Magnetolectric stimulation**

The development of ES devices for deep brain modulation has indeed brought about significant advancements in the treatment of neurological and psychiatric disorders. However, early devices had limitations such as their size, surgical implantation requirement, and wired power, which increased the risk of complications and limited the patients' mobility and daily activities. One solution to address these limitations is the MagnetoElectric-powered Bio ImplanT (ME-BIT) technology. Unlike miniature ultrasound-driven devices that require ultrasound gels or foams for power transfer, ME-BIT devices can maintain power levels over a wider range of translational and angular misalignments without the need for such coupling agents. ME-BIT operates on the principle of electromagnetic (EM) induction, allowing for wireless neurostimulation by delivering EM stimulation through body tissues. However, there are challenges in power transmission using EM waves, as it requires antennas with feature sizes comparable to the wavelengths of the EM waves. For sub-millimeter devices, the effective frequency of EM radiation falls in the GHz range, which can be absorbed by the body, thereby limiting the safe amount of power that can be transmitted to deep tissue implants. This often necessitates placing the implants closer to the skin surface<sup>[37]</sup>. To overcome this limitation, researchers have turned to near-field inductive coupling (NIC) for driving implanted devices. However, miniaturization of the receiver coil can lead to a decrease in output power due to reduced capture flux. Additionally, small changes in the distance or angle between the transmitter and receiver can significantly impact the function of these miniaturized devices<sup>[38-40]</sup>. The development of more advanced and miniaturized EM stimulation devices with improved power



transmission efficiency and stability remains an ongoing area of research. By addressing these challenges, researchers aim to enhance the safety and effectiveness of DBS devices for the treatment of neurological and psychiatric disorders.

Magnetolectric (ME) materials enable the possibility of miniaturizing and remotely powering neural stimulators. Similar to inductive coils, these materials convert magnetic fields into electric fields by mechanically coupling the magnetostrictive layer and the piezoelectric layer in thin films. When the magnetic dipoles align with the external field, strain is generated in the magnetostrictive layer, exerting a force on the piezoelectric layer and resulting in a voltage. Selective activation of the film is possible by designing multiple films to vary the stimulation frequency. ME materials offer two main advantages: firstly, stable and effective excitation can be achieved as the device becomes smaller and moves relative to the drive coil; secondly, the voltage generated by the piezoelectric material depends on the thickness of the piezoelectric layer rather than its area, enabling the fabrication of small ME films.

**Figure 3A** illustrates the application of a wireless Magnetostrictive-Elastic stimulator for delivering therapeutic DBS in a freely moving rodent model with Parkinson's disease. This demonstrates the precise control of neuronal activity through ME stimulation<sup>[41]</sup>. To enhance control over the magnitude and frequency of the voltage generated by the ME material, Yu *et al.* integrated the ME material with a System-on-Chip (SoC) to create a wireless programmable neurostimulator for data transmission. This integration includes an SoC with an embedded ME transducer, a single energy storage capacitor, and an electrode on a flexible polyimide substrate<sup>[42]</sup>. Building upon this, Chen *et al.* introduced a wireless millimetric ME implant for endovascular stimulation of peripheral nerves. As depicted in **Figure 3B**, this implant successfully stimulated specific peripheral nerves that were challenging to access through conventional surgery. The device can transmit stimuli via a percutaneous catheter and receive data and power using the SoC. The implant utilizes a stacked bilayer material composed of MetGlas (magnetostrictive layer) and lead zirconium titanate (PZT) (piezoelectric layer). The entire wireless ES system comprises an external magnetic field transmitter, an ME film for deriving energy and data from the magnetic field, and a custom integrated circuit (IC) for interpreting digital data and generating the ES delivered by the electrodes. Additionally, the ME-BIT is enclosed within a customized three-dimensional (3D) printed PLA capsule. It demonstrated that when wirelessly powered ME-BITs came into contact with the sciatic nerve, they could consistently evoke compound muscle action potentials (CMAP) with observable leg movements. ME-BITs possess the capability to modulate stimulus amplitude within a range of 0.3 to 3.3 V. Moreover, they can adjust pulse widths and frequencies to cater to various neuromodulation applications and provide targeted therapies<sup>[43]</sup>.

*In vivo* studies conducted in mice revealed that ME nanoparticles can directly link the intrinsic neural activity electric field with an external magnetic field<sup>[44]</sup>. Building upon this finding, Kozielski *et al.* introduced the concept of an injectable ME nano-electrode (MENP). This MENP can wirelessly transmit electrical signals to the brain in response to external magnetic fields. Notably, this regulatory mechanism does not necessitate genetic modification of neural tissue, allowing the animal to move freely during stimulation. The two-phase MENPs were constructed using magnetostrictive  $\text{CoFe}_2\text{O}_4$  (CFO) nanoparticles coated with piezoelectric  $\text{BaTiO}_3$  (BT)<sup>[45]</sup> [**Figure 3C**]. These MENPs were stereotactically implanted into the hypothalamic region of freely moving mice and powered by an external magnetic field. The results indicate that modulation of the local thalamic subthalamic region promotes modulation of other regions connected through the basal ganglia circuit, resulting in behavioral changes in the mice. Furthermore, the output of the MENPs exhibits only a minor dependence on the frequency of the input carrier alternating current (AC) field. It can effectively locally modulate neuronal activity both *in vitro* and *in vivo* using non-resonant magnetic power.

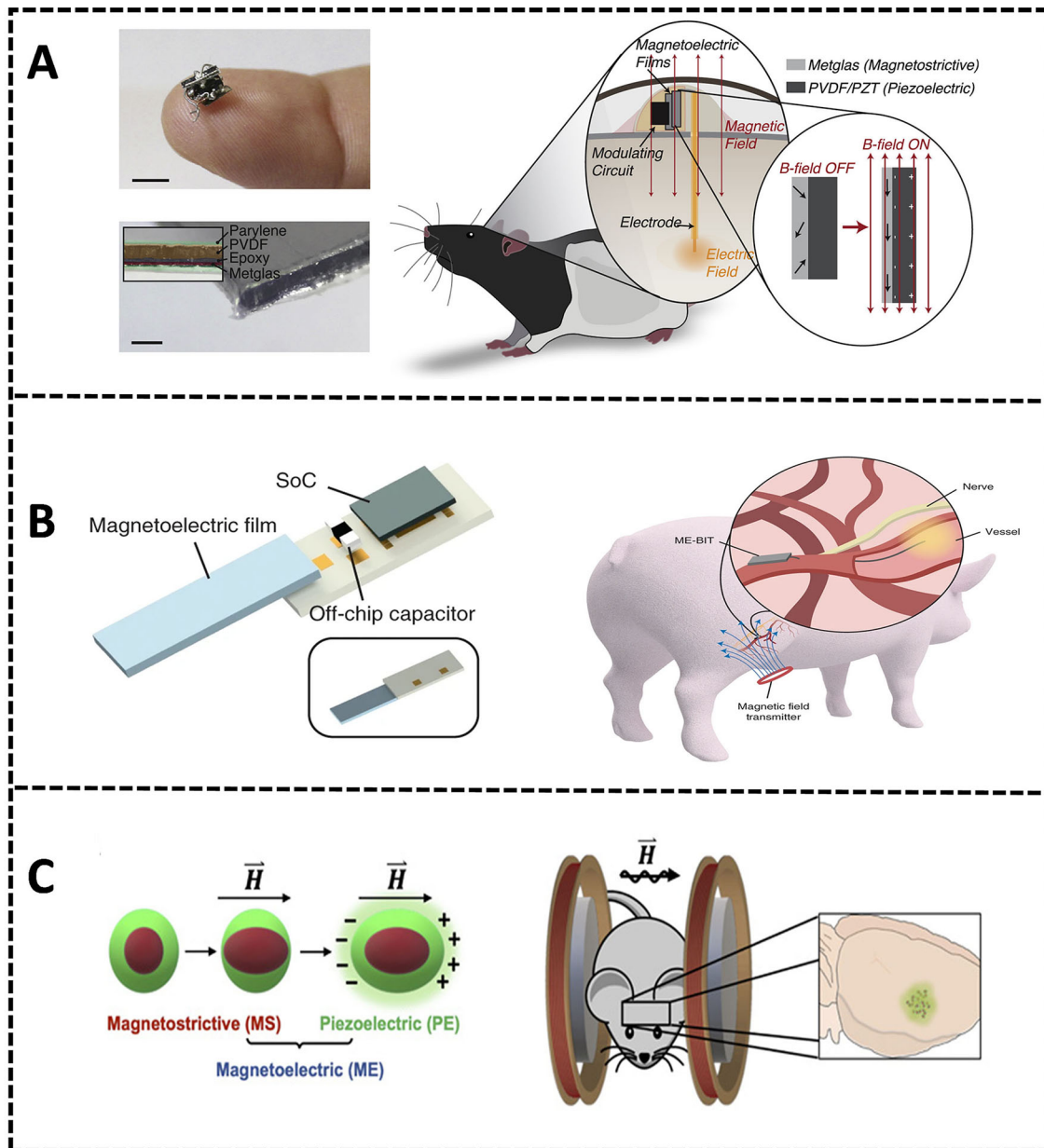


**Figure 3.** (A) Wireless neurostimulator based on ME material<sup>[41]</sup>. Reprinted with permission. Copyright 2020, Elsevier; (B) Wireless programmable neurostimulator for stimulation of perivascular nerves<sup>[43]</sup>. Reproduced with permission. Copyright 2022, Springer Nature; (C) Injectable ME nano-electrodes<sup>[45]</sup>. Reproduced with permission. Copyright 2021, AAAS. ME-BIT: MagnetoElectric-powered Bio Implant; PVDF: polyvinylidene fluoride; PZT: lead zirconium titanate.

The researchers discovered that in the presence of a primary coil, wireless ES can be achieved through EM induction. This is accomplished using a conductive annular graphene substrate, which was grown through chemical vapor deposition and serves as a secondary coil [Figure 4A]. Notably, this substrate is biocompatible for the cultivation of neural stem cells (NSCs).

The application of wireless ES was observed to enhance neuronal differentiation and the development of neural protrusions without causing significant effects on the viability and overall maintenance of NSCs<sup>[46]</sup>.



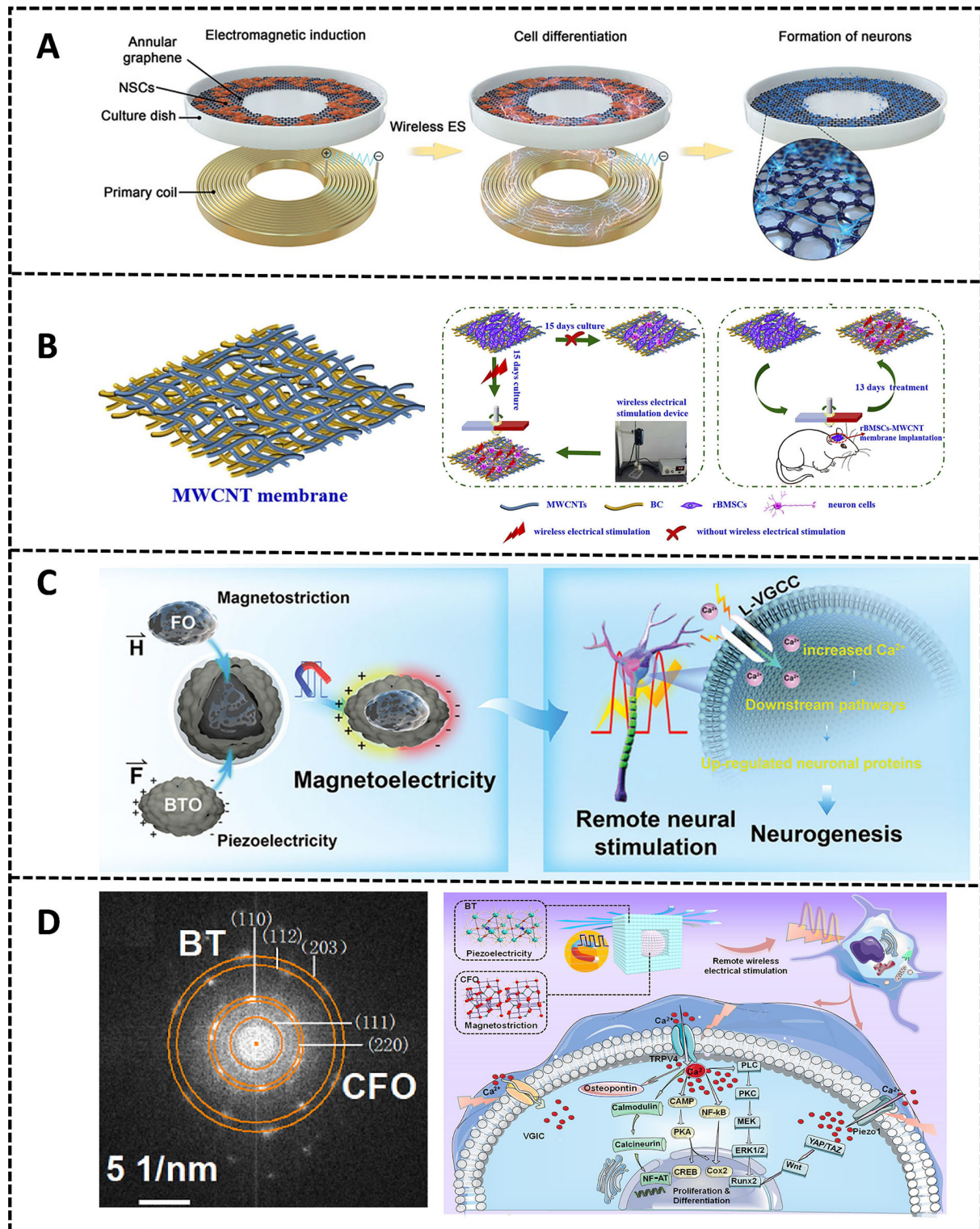


**Figure 4.** (A) Conductive annular graphene substrate<sup>[46]</sup>. Reprinted with permission. Copyright 2021, John Wiley & Sons, Inc; (B) Highly conductive flexible multi-walled carbon nanotube membrane<sup>[8]</sup>. Reprinted with permission. Copyright 2022, Elsevier; (C)  $Fe_3O_4@BaTiO_3$  nanoparticles-loaded hyaluronic acid/collagen hydrogel<sup>[48]</sup>. Reprinted with permission. Copyright 2021, John Wiley & Sons, Inc; (D) CFO and BT core-shell structured nanoparticles<sup>[49]</sup>. Reprinted with permission. Copyright 2022, Elsevier. BT:  $BaTiO_3$ ; CFO:  $CoFe_2O_4$ ; MWCNT: multi-walled carbon nanotube; NSCs: neural stem cells; rBMSCs: rat bone marrow mesenchymal stem cells.

Subsequently, a wireless-triggered local ES system was developed. This system utilized a highly conductive, flexible MWCNT membrane combined with a rotating magnetic field to induce the specific differentiation of bone marrow-derived cells in rats. MWCNTs possess properties akin to neural structures, such as dendrites, making them promising candidates for nerve regeneration techniques and broader biomedical applications. To achieve this, CNT conductive flexible membranes were created by blending MWCNTs with bacterial cellulose nanofibers<sup>[8]</sup> [Figure 4B]. Neural differentiation was facilitated by positioning a rotating magnetic field outside the MWCNT conducting membrane, which had been implanted in rat bone marrow mesenchymal stem cells (rBMSCs). Local ES, carried out on the highly conductive, flexible MWCNT membranes, was triggered by the rotating magnetic field. This stimulation was transmitted to the cells through direct contact between the cells and the nanofiber membrane's surface, resulting in the differentiation of rBMSCs into neuronal cells. *In vivo* experiments conducted on male rats affirmed the beneficial effects of wireless ES in regulating rBMSCs, thereby holding promise for neural repair.

Tang *et al.* designed CFO/P(VDF-TrFE) nanocomposite films by combining magnetostrictive CFO nanoparticles with a piezoelectric P(VDF-TrFE) matrix. Their investigation revealed that cells cultured on the nanocomposite film exhibited periodic responses at different time points through the dynamic temporal modulation of the magnetic field<sup>[47]</sup>. Then, Zhang *et al.* developed core-shell-structured Magnetostrictive-Elastic Fe<sub>3</sub>O<sub>4</sub>@BT nanoparticles loaded into hyaluronan/collagen hydrogels<sup>[48]</sup> [Figure 4C]. They demonstrated that ME stimulation facilitated both cellular-level neurogenesis and *in vivo* recovery from spinal cord injuries. Qi *et al.* cultivated piezoelectric BT directly on magnetostrictive CFO to produce core-shell-structured nanoparticles. These nanoparticles were subsequently integrated into poly(lactic acid) [Poly (L-lactic acid), PLLA] scaffolds, which are naturally biodegradable and break down completely into water and carbon dioxide in a bodily fluid environment. Additionally, the CFO cores had the capacity to generate strain in response to an applied magnetic field driven by the movement and rotation of magnetic domains. This strain was transmitted to the BT shell layer through interfacial coupling, causing structural changes in BT domains and resulting in the generation of electrical signals. This approach established a non-invasive ES system. They substantiated that ME signals effectively promoted cell proliferation and differentiation, upregulating the expression of genes such as COL-I, OCN, and Runx2, among others<sup>[49]</sup> [Figure 4D].

### Photoelectric stimulation

In wireless devices for ES, the miniaturization, lightweight design, energy supply and storage, and electrode biocompatibility pose significant challenges, restricting their long-term functionality and application potential. Photovoltaic power generation, which converts light energy into electrical energy, offers a solution to the power supply challenge faced by electrical devices. The photovoltaic effect arises from the exposure of a non-uniform semiconductor to light, resulting in the separation of electron-hole pairs due to its asymmetric structure, which, in turn, creates a potential difference and establishes an internal electric field. The flexible photovoltaic ES device, comprising novel materials with excellent biocompatibility, can be directly applied to the targeted stimulation area. By utilizing wireless EM transmission, visible or near-infrared light is converted into electrical signals to provide limitless electrical power for neural stimulation on these flexible devices. This approach reduces the biological harm associated with conventional electrodes and lays the groundwork for miniaturization and lightweight design. Presently, photodiodes serve as the primary technology employed in this type of flexible photovoltaic ES device. When a sufficient number of energetic photons impinge upon the photodiode's PN-junction, its asymmetric structure generates hole-electron pairs, resulting in the production of photocurrent.

Retinal degenerative diseases, characterized by the progressive loss of retinal pigment epithelial cells and photoreceptor cells, are a major cause of blindness. This results in the gradual deterioration of visual function until complete blindness occurs. Silicon photodiodes, which can efficiently convert light pulses

into electrical pulses, are a well-established technology that has been extensively researched for their applications in neuronal stimulation, particularly in the development of artificial retinal prostheses. Flexible photovoltaic ES devices, which are based on the photovoltaic effect, are commonly implanted on the retinal surface. These devices sense light, convert it into electric current, stimulate the optic nerve, and induce visual perception. Additionally, they can be used for the treatment of retinal degenerative diseases<sup>[50-52]</sup>. Photovoltaic retinal prostheses have proven to be an effective approach for restoring visual function in patients suffering from retinal degenerative blindness.

Palanker *et al.* have conducted a series of exploratory studies on the use of silicon photodiodes to stimulate the visual nerve of the retina. In 2006, they proposed a design for a high-resolution photovoltaic retinal prosthesis system. The fundamental concept involves implanting a small, wireless, flexible device that contains silicon photodiodes into the retina. This device can directly project images onto the silicon photodiodes using near-infrared light. In the extracellular region, the silicon photodiodes convert light into pulsed microcurrents. These microcurrents stimulate the optic nerve, activate photoreceptor cells, and restore vision<sup>[9]</sup>. [Figure 5A](#) depicts the three main components of the system: (a) the image projection component, which employs an infrared LED-LCD display on goggles to project the image onto the flexible device within the retina in a collimated manner. This eliminates the need for complex electronic equipment and wiring schemes while also minimizing the loss of incident light and facilitating the generation of current on the charged photodiodes of the activated device; (b) the photoelectric conversion component, which converts light into pulsed current through the photodiodes; and (c) the calibration and tracking component, which detects pupil-reflected light or LED-emitted backlight using a tracking array that is aligned with the LCD display plane. This enables image perception and dynamic capture. The technology has the theoretical capability to perform dynamic scanning at various levels of brightness, thereby restoring normal vision through the ES of the surviving neurons.

Loudin *et al.* discovered that the linear conversion width, which defines the dynamic range of stimulation current that can be delivered by a retinal prosthesis, plays a significant role in converting light linearity to current in silicon photodiodes. Based on this discovery, they designed and created a wireless flexible device using photolithography and deposition techniques<sup>[53]</sup>. The device, as illustrated in [Figure 5B](#), features a columnar surface structure to enhance biocompatibility and integrates a silicon photodiode into the SU-8 substrate. Preliminary biological tests indicated that the retinal tissues successfully adhered to the flexible device without significant damage and moved toward the columns, suggesting that the retinal structure remained largely unchanged. However, the column design reduces the feasibility of hermetically sealing the electrode fibers. Further research is needed to identify optimal strategies for enhancing device biocompatibility and encapsulation compatibility and fully understand the system's overall functionality.

Mathieson *et al.* conducted comprehensive research on the existing device and performed advanced biological experiments<sup>[54]</sup>. The image projection component utilizes pulsed near-infrared light (880-915 nm) to project images onto the flexible photovoltaic ES device positioned beneath the retina. This component generates pulsed light with adequate intensity to drive the photodiode array effectively while remaining imperceptible to any remaining photoreceptors. The photodiode array beneath the retina converts these light signals into pulsed photocurrents in a linear fashion. Iridium oxide electrodes transmit these stimulation pulses to the retina, primarily targeting<sup>[54]</sup> the surviving cells in the inner nuclear layer (INL) [[Figure 5C](#)]. Two distinct silicon photodiode arrays were designed: (A) a square array, each diode having a photosensitive area of approximately  $25\ \mu\text{m} \times 25\ \mu\text{m}$ , known as a photosensitive pixel. Each photosensitive pixel has an iridium oxide stimulation electrode of approximately  $10\ \mu\text{m} \times 10\ \mu\text{m}$  at its center (illustrated as "1"). Additionally, all diodes share a common return electrode situated on the backplane of the array; (B) A



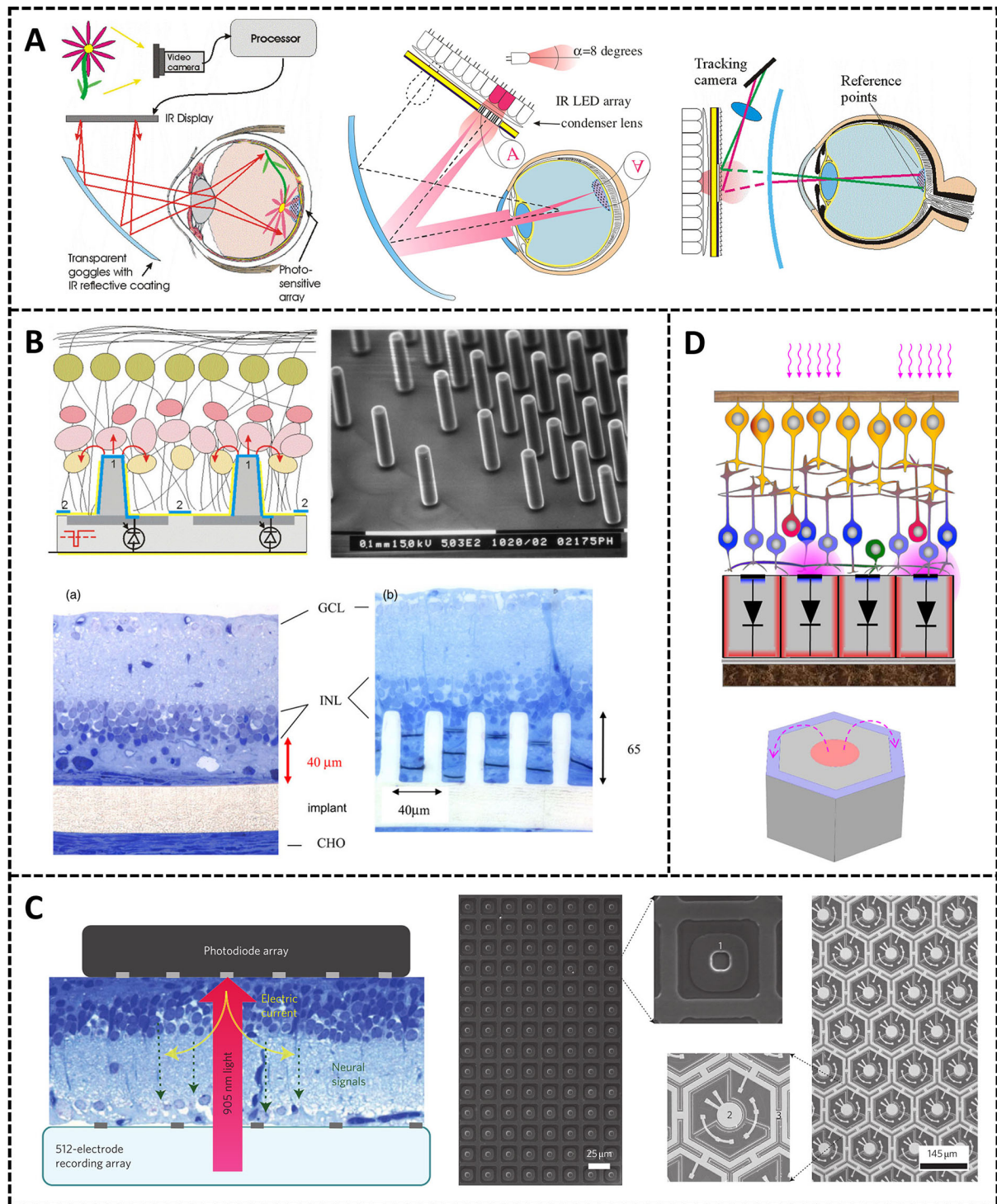


**Figure 5.** Flexible photovoltaic electrical stimulation device based on silicon photodiodes. (A) High-resolution photovoltaic retinal prosthesis system, including image projection part, photoelectric conversion part, and calibration and tracking part<sup>[9]</sup>. Reprinted with permission. Copyright 2005, IOP Publishing; (B) Silicon photodiodes are packaged with SU-8, and columnar structures are designed to improve the biocompatibility of the device<sup>[53]</sup>. Reprinted with permission. Copyright 2007, IOP Publishing; (C) Two different silicon photodiode arrays are designed: square and hexagonal<sup>[54]</sup>. Reprinted with permission. Copyright 2012, Springer Nature; (D) A planar monopolar photosensitive pixel structure is designed to reduce the size to 20  $\mu\text{m}$ <sup>[58]</sup>. Reprinted with permission. Copyright 2022, Springer Nature. IR: Infrared; GCL: ganglion cell layer; INL: inner nuclear layer; CHO: choroids.

hexagonal array, where each hexagon consists of three series-connected diodes. The central diode (illustrated as “2”) has an iridium electrode and is surrounded by a common return electrode (illustrated as “3”). Two devices were fabricated, with photosensitive areas of 70 and 140  $\mu\text{m}$ , respectively. The center electrode diameters were 20 and 40  $\mu\text{m}$ , and each hexagon was separated by a 5  $\mu\text{m}$  groove. The square diode array can generate a maximum of 0.5 V under physiologically safe light pulses, successfully stimulating the retina. In contrast, the hexagonal diode array can safely apply higher voltages under physiological conditions.

The group is dedicated to investigating photovoltaic retinal prosthesis devices with high resolution and compactness. Boinagrov *et al.* developed a computational model to optimize the system for maximum charge injection under various light intensities and stimulation thresholds. The model incorporates photoelectric current dynamics and utilizes circuit simulation and other methods<sup>[55]</sup>. Calculations have demonstrated that the number of diodes per photosensitive pixel should not exceed 3, with the optimal number depending on the required charge. Thus, it may vary across different applications. Lei *et al.* introduced a new array<sup>[56]</sup> that features optimized pixel configuration and reduced size based on the hexagonal array. The primary approach involves using ultra-thin isolation trenches to separate the diodes within the photosensitive pixel from adjacent pixels. Additionally, the return electrode is shared between adjacent pixels to enhance the effective area of the photodiode. Research has demonstrated that arrays with pixel sizes as small as 40  $\mu\text{m}$  can elicit retinal responses under safe conditions of near-infrared light (880 nm). As the pixel size decreases, the threshold increases, aligning with the decrease in current and the more stringent limitation of the electric field between the active electrode and the return electrode. By implanting larger or multiple modules, the number of pixels can be increased to thousands, thereby establishing the groundwork for restoring high visual acuity. The size of photosensitive pixels in hexagonal arrays has been reduced to 40  $\mu\text{m}$  under safe stimulation conditions.

In 2D devices, the stimulation threshold increases with decreasing size of photosensitive pixels. When the size of photosensitive pixels is less than 40  $\mu\text{m}$ , the stimulation threshold exceeds the charge injection limit of the electrodes. Moreover, excessive crosstalk between adjacent electrodes within each photosensitive pixel limits the effective electric fields, thereby preventing effective stimulation of subretinal pixels smaller than 55  $\mu\text{m}$ . Bhuckory *et al.* developed a 3D honeycomb photovoltaic prosthesis with 10  $\mu\text{m}$  wide holes, building upon a 40  $\mu\text{m}$  device. The honeycomb structure will create an almost uniform vertical electric field, substantially reducing the stimulation threshold of the device independent of the width of photosensitive pixels. When a single retinal cell enters a honeycomb electrode hole, it will encounter an almost uniform vertical electric field, leading to a significant reduction in the stimulation threshold and enabling single-cell stimulation of the retina<sup>[57]</sup>. Wang *et al.* proposed a high-resolution photovoltaic retinal prosthesis design that is implanted beneath the retina using a planar monopolar configuration<sup>[58]</sup>. As depicted in [Figure 5D](#), the electric field within the photosensitive pixels of this device is predominantly vertical. The stimulation threshold for a 10 ms pulse is approximately 0.06  $\text{mW}/\text{mm}^2$ , which is 30 times higher than that of a 40  $\mu\text{m}$  bipolar pixel (1.8  $\text{mW}/\text{mm}^2$ ). Additionally, with this approach, the pixel size can be reduced to 20  $\mu\text{m}$  (matching the natural visual acuity limit of 28  $\mu\text{m}$  in rats) without being constrained by the pixel spacing. A 20  $\mu\text{m}$  pixel has the potential to restore central vision to 20/80 for AMD patients, thereby holding considerable clinical implications.

The retinal stimulation technology based on silicon photodiodes has now reached the clinical trial stage. During visual nerve stimulation, a flexible photovoltaic ES device is implanted beneath the retina, allowing light to pass through translucent tissue without harm and be directed toward the device. However, when implanted under the skin or other tissues, the presence of opaque tissues can obstruct the transmission of

light, resulting in the device's inability to deliver a consistent current for effective nerve stimulation. One of the challenges that needs to be addressed is how to generate ES by activating the device with minimal light.

Organic photoelectric capacitors are currently a prominent research focus in flexible photovoltaic ES devices, offering potential solutions to the aforementioned challenges. The organic photoelectric capacitor is essentially a photodiode, functioning based on the photovoltaic effect. It possesses an organic material p-n junction that becomes activated by light and can generate a sufficiently strong current to stimulate non-transparent tissues for neurostimulation. Rand *et al.* at Brno University of Technology have been dedicated to the study of organic optoelectronic devices<sup>[12,59,60]</sup>. Rand *et al.* optimized existing brain nerve stimulation approaches, beginning with organic materials, and introduced a highly efficient nanoscale semiconductor photoelectric system known as the organic electrolytic photocapacitor (OEPC)<sup>[12]</sup>. As depicted in [Figure 6A](#), it essentially consists of a photodiode with a three-layer thin film structure comprising Cr/Au and p-n semiconductor organic nanocrystals with a thickness of 80 nm. When pulsed light is applied to the device immersed in physiological saline, electrons accumulate in the n-type semiconductor layer, while photo-generated holes are injected into the metal. Upon charging the device, pulsed light is transformed into a localized displacement current, which is sufficiently powerful to safely stimulate neurons when interacting with organic materials. Through calcium imaging tests, they verified the capacity and stability of organic photoelectric capacitors in eliciting action potentials under physiological conditions and provided preliminary evidence of their non-destructive impact on cell viability. Being the first non-silicon optoelectronic platform with the ability to generate photovoltages and displacement currents of adequate magnitude for cell stimulation, this device holds the potential to enhance the photoelectric conversion efficiency of flexible photovoltaic ES devices.

To optimize the efficiency of OEPC, it is necessary to enhance the transport of effective capacitor charge. On this basis, Silverå Ejneby *et al.* achieved a significant enhancement in the photovoltaic stimulation performance of OEPC devices by employing conductive polymer PEDOT:PSS coatings<sup>[59]</sup>. [Figure 6B](#) illustrates the enhancement process. In order to promote strong adhesion of subsequent organic semiconductor layers, indium tin oxide (ITO) was chosen as the substrate for OEPC. The deep blue regions in Type II and Type III indicate the presence of the deposited PEDOT:PSS coating. This modification resulted in a 2-3 times increase in the charge density of the photoelectrode, leading to a significant improvement in the stimulation performance of OEPC. Additionally, it reduced the interfacial impedance and provided insights for the miniaturization design of OEPC.

The following year, Silverå Ejneby *et al.* conducted comprehensive biological experiments involving OEPC<sup>[60]</sup> [[Figure 6C](#)]. A flexible ultra-thin structure incorporating OEPC was developed to construct a self-locking sleeve band, which was subsequently implanted into a live rat. Deep infrared pulsed light is employed to irradiate the mice, enabling communication with and activation of the implanted OEPC. This is facilitated by the ability of deep infrared light to penetrate the skin, fat, and other tissues. The findings demonstrated that the photoelectric charging and discharging behavior of the OEPC stimulation device successfully activated the sciatic nerve in live rats. Furthermore, precise control of sciatic nerve stimulation was achieved by adjusting the intensity and duration of pulsed light. The implantation of the device did not impede the mice's physiological movement behavior, and the stimulation operation remained effective for a duration of up to three months following implantation. The ultra-thin organic photoelectric capacitor OEPC has a total volume of 0.1 mm<sup>3</sup> and can be integrated into a wireless flexible photovoltaic device. This device is capable of generating adequate *in vivo* charge to achieve neural stimulation, thereby offering a viable approach for achieving non-transparent *in vivo* neural stimulation.



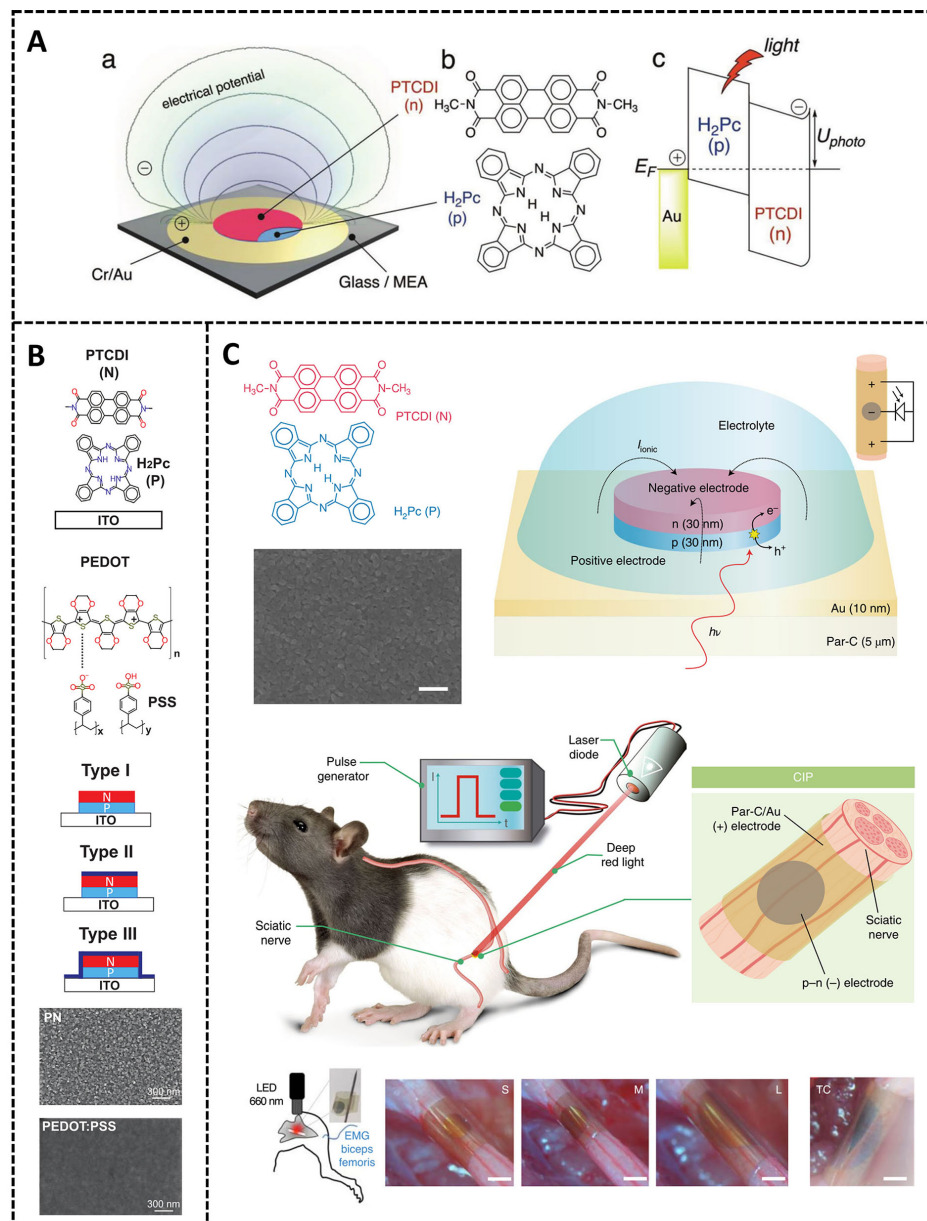


**Figure 6.** Flexible photovoltaic electrical stimulation device based on organic photoelectric capacitors. (A) Schematic diagram of a photoelectric capacitor composed of sequentially deposited Cr/Au and H<sub>2</sub>Pc (p-type) and PTCDI (n-type)<sup>[12]</sup>. Reprinted with permission. Copyright 2018, John Wiley and Sons; (B) Schematic diagrams of three OEPC devices, p-type: H<sub>2</sub>Pc (P), n-type: PTCDI, and the blue overlay in type II and type III represents the PEDOT:PSS coating<sup>[59]</sup>. Reprinted with permission. Copyright 2020, John Wiley and Sons; (C) OEPC achieves wireless stimulation of the sciatic nerve in mice<sup>[60]</sup>. Reprinted with permission. Copyright 2022, Nature Research. EMG: Electromyography; ITO: indium tin oxide; MEA: monoethanolamine; OEPC: organic electrolytic photocapacitor; PEDOT: poly(3,4-ethylenedioxythiophene); PEDOT:PSS: poly(3,4-ethylenedioxythiophene)-poly(styrenesulfonate); PN: photoconductor nanocrystalline; PTCDI: photoconductor nanocrystalline.

Organic photoelectric capacitors have significantly enhanced the photoelectric conversion efficiency and stimulation effectiveness of flexible photovoltaic ES devices. This expansion of their application scope holds great potential for their utilization in clinical medical treatments for nervous system diseases, making it a key area of future development.

### Ultrasound-driven electrical stimulation

Ultrasound, as a mechanical wave with a frequency exceeding 20 kHz, has the capability to penetrate biological tissues and transmit energy. To achieve a wireless power supply, a novel strategy for ultrasound energy harvesting is proposed. This process involves the transmission of ultrasound waves from an external source into the body, followed by the utilization of an energy harvester to convert the ultrasound into electricity. This type of electrical stimulator, driven by ultrasound, has the capability to activate nerve cells. The use of ultrasound-driven electrical nerve stimulation has several key benefits. First, ultrasound exhibits excellent directionality in biological tissues and enables penetration to a depth of a few centimeters. Additionally, the speed of sound in tissues is five orders of magnitude lower than that of radio waves, which enables the energy to be concentrated in a small area, resulting in high spatial resolution<sup>[61]</sup>; Second, the attenuation of acoustic energy in tissues is much smaller than that of EM radiation, allowing for higher energy conversion efficiencies and reduced scattering<sup>[62]</sup>; Third, ultrasound generally exhibits a superior safety profile for biomedical applications. Ultrasound technology has long been utilized in medical diagnosis and treatment. The U.S. Food and Drug Administration (FDA) allows a limited ultrasound intensity of  $720 \text{ mW}\cdot\text{cm}^{-2}$  to be used in diagnostic applications, which is significantly higher than the safety threshold of radio waves in the human body<sup>[37,63]</sup>. Therefore, ultrasound serves as an ideal energy source for wirelessly powering, exciting, and modulating implantable bioelectric stimulation devices.

Piezoelectric materials, as dielectric materials, experience strain when subjected to mechanical stress along a specific direction. This strain leads to internal polarization, separating positive and negative charge centers and inducing the formation of electric dipole moments. The crystal structure of piezoelectric materials is non-centrosymmetric, allowing for the accumulation of opposing charges on two opposing surfaces, which generates a piezoelectric potential. Hence, piezoelectric materials have the capability to convert energy into electrical energy, making them an ideal candidate for ultrasound electrical stimulators. To enhance their piezoelectric performance and energy harvesting efficiency, two key approaches are employed: improved material selection and structural design.

Due to their small size and unique electrical properties, piezoelectric nanomaterials are capable of harvesting ultrasonic energy and generating sufficient electrical power over a given distance. Wang *et al.* pioneered the development of a nanogenerator based on ZnO nanowires (NWs)<sup>[64]</sup>. After placing vertically aligned ZnO nano-arrays underneath the serrated electrodes, they utilized ultrasound to induce the bending or vibration of electrodes and NWs, successfully converting the latent mechanical energy of ultrasonic waves into electrical energy [Figure 7A]. Ciofani *et al.* cocultured neuron-like P12 cells with boron nitride nanotubes (BNNTs) and performed mechanical stress on them through ultrasound<sup>[65]</sup>. The polarization induced by the piezoelectric properties of BNNTs under stress affects the inward flow of calcium ions and creates a potential difference, enabling ES to the neuronal cells [Figure 7B]. Calcium ions play an important role in the growth of P12 neural protrusions, and a significant enhancement of neural protrusion development under ultrasound-driven BNNT stimulation was once observed. Next, Marino *et al.* provided indirect ES to SH-SY5Y neuron-like cells using tetragonal barium titanate nanoparticles (BTNPs)<sup>[66]</sup> [Figure 7C]. Piezoelectric BTNPs were bonded to the cytoplasmic membrane and caused the plasma membrane to depolarize, activating voltage-gated  $\text{Na}^+$  channels and  $\text{Ca}^{2+}$  channels. As a result, high-amplitude  $\text{Ca}^{2+}$  transients are generated, ultimately triggering neuronal activity. Currently, there is a growing number of nanogenerators being developed from diverse materials and in various forms. With their performance continually improving, such devices have the potential to be applied in various areas of spatially confined neural stimulation.

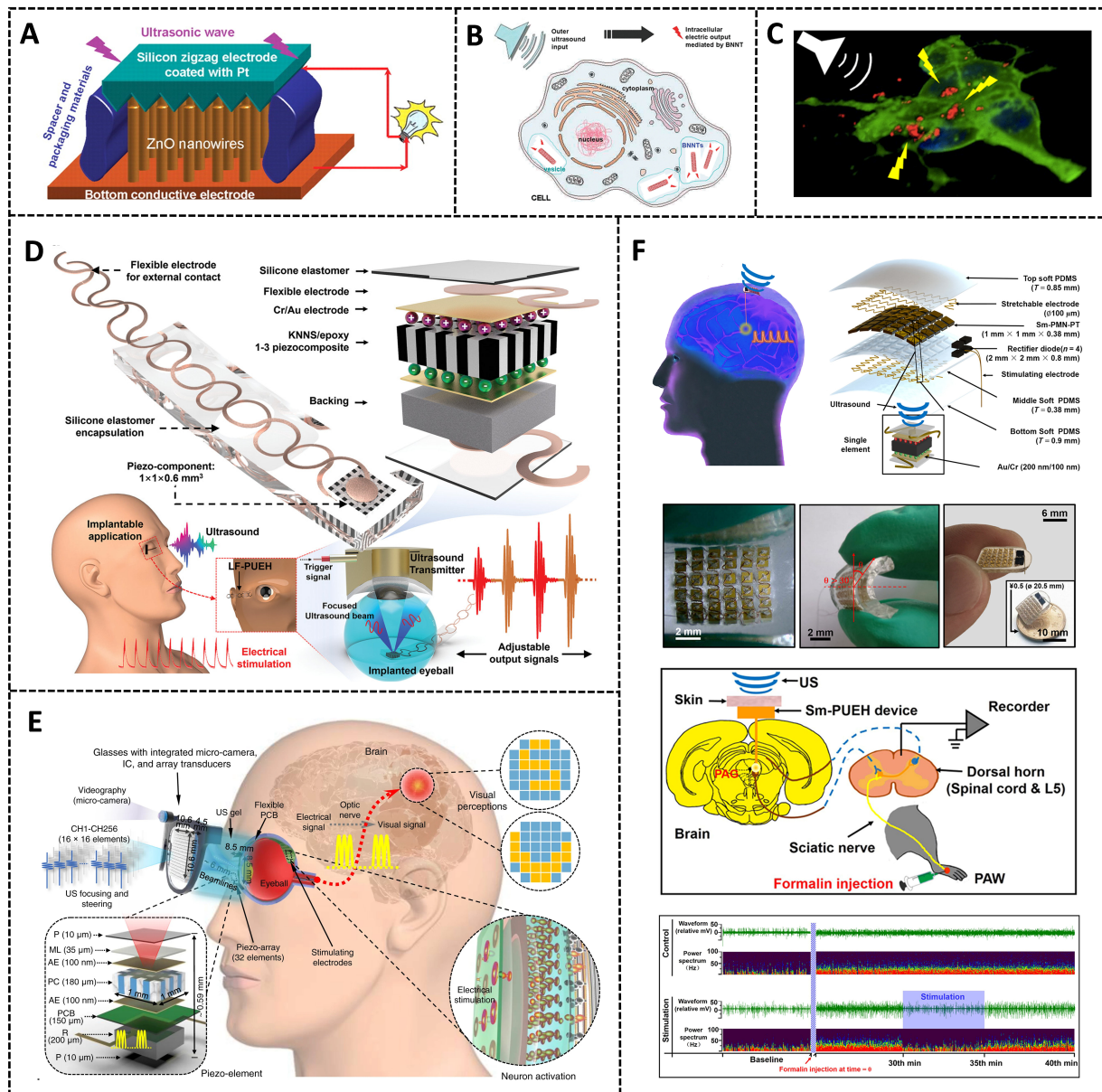


**Figure 7.** Wireless neurostimulation using an ultrasound-driven nanogenerator and ultrasound energy harvesting device. (A) ZnO nanogenerator<sup>[64]</sup>. Reprinted with permission. Copyright 2007, The American Association for the Advancement of Science; (B) BNNTs for ultrasound-driven electrical stimulation<sup>[65]</sup>. Reprinted with permission. Copyright 2010, American Chemical Society; (C) BTNPs for ultrasound-driven electrical stimulation<sup>[66]</sup>. Reprinted with permission. Copyright 2015, American Chemical Society; (D) LF-PUEH to produce retinal neurostimulation<sup>[71]</sup>. Reprinted with permission. Copyright 2019, John Wiley and Sons; (E) F-URSP arrays as visual prosthesis<sup>[72]</sup>. Reprinted with permission. Copyright 2022, Springer Nature; (F) PUEH arrays for stimulation of PAG<sup>[10]</sup>. Reprinted with permission. Copyright 2021, AAAS. AE: Au/Cr electrode; BNNTs: boron nitride nanotubes; BTNPs: barium titanate nanoparticles; F-URSP: flexible US-induced retinal stimulating piezo-array; ML: matching layer; LF-PUEH: lead-free piezoelectric ultrasonic energy harvester; PAG: periaqueductal gray; PAW: periaqueductal gray; PC: piezo-composite; PCB: printed circuit board.

After confirming the feasibility of ultrasound-driven ES, researchers have investigated various composite materials to improve their piezoelectric properties, flexibility, and biocompatibility for efficient implantable neural stimulation. Piezoelectric ceramic materials are employed for electroacoustic conversion because of their simple preparation process and outstanding acoustic and electrical properties. These materials exhibit strong responsiveness to ultrasound and can induce neural activity. Piech *et al.* presented an implantable

neurostimulator that is wireless, lead-free, and battery-free based on a lead zirconate titanate (PZT) piezoelectric ceramic transducer<sup>[67]</sup>. The designed system consists of a piezoelectric ceramic transducer, an energy storage capacitor, and an IC. When implanted in the sciatic nerve of an anesthetized rat, the device consistently generates electrical neurostimulation across a range of physiological responses. Additionally, an ultrasonic source and an external transceiver provide power and enable bi-directional communication, indicating potential for future advancements in neural interface technologies.

However, piezoelectric ultrasound energy-harvesting (PUEH) devices made from materials such as PZT films, PZT 1-3 composites, and so on exhibit low energy density<sup>[10,68-72]</sup>. Jiang *et al.* reported a PZT 1-3 composite-based PUEH device, which is encapsulated in flexible silicone elastomers with a millimeter size<sup>[71]</sup> [Figure 7D]. In a proof-of-concept demonstration, the developed device was surgically implanted into isolated pig eyes, resulting in neural stimulation that surpassed the conventional threshold for retinal stimulation. This breakthrough expands the potential application of ES in essential medical procedures. Then, they utilized PZT 1-3 composite to fabricate a flexible US-induced retinal stimulating piezo-array. Such a device integrates a 2D piezoelectric array with 32-pixel stimulating electrodes in a flexible printed circuit board for direct contact with the retina<sup>[72]</sup> [Figure 7E]. Each piezoelectric element can be activated individually by ultrasound. A 256-array 2D ultrasound array transducer is used to generate programmable ultrasound beamlines, which, in turn, activate neural receiver pixels and reconstruct the electronic pattern, thereby providing an artificial visual prosthesis.

With the emergence of new piezoelectric materials, there has been a significant improvement in the performance of PUEH devices. As shown in Figure 7F, our group<sup>[10]</sup> designed and fabricated a wireless and flexible implantable neurostimulator based on Sm-doped  $\text{Pb}(\text{Mg}_{1/3}\text{Nb}_{2/3})\text{O}_3$ - $\text{PbTiO}_3$  single crystals for analgesia. The entire device is a  $6 \times 6$  elements array with dimensions of  $13.5 \text{ mm} \times 9.6 \text{ mm} \times 2.1 \text{ mm}$ , weighs only 0.78 g, and is biocompatible. Such a device can generate up to  $1.1 \text{ W/cm}^2$  instantaneous power density and  $4,270 \pm 40 \text{ nW}$  average charging power in vitro, and after implantation into the rat brain, it can generate an instantaneous effective output power of  $280 \text{ }\mu\text{W}$  under the effect of  $1 \text{ MHz}$  ultrasound at  $212 \text{ mW/cm}^2$ . Most importantly, it can immediately activate the periaqueductal gray (PAG) region of the brain, achieving pain inhibition.

As is known, traditional piezoelectric materials contain toxic components. Taking into account safety aspects, it is essential to explore new neurostimulators based on environment-friendly piezoelectric materials. As illustrated in Figure 8A, Jiang *et al.* proposed a 3D twinning wireless implantable ultrasound-driven ES system using  $(\text{K},\text{Na})\text{NbO}_3$ -based materials, which combines the advantages of high spatial and temporal resolution, high power output, and flexible directionality<sup>[73]</sup>. The developed device employs a bio-inspired 3D twinning array that allows 3D twinning on the surface of the target tissue, enabling multi-angle energy capture. Chen *et al.* utilized electrostatic jet printing to fabricate a composite of polyvinylidene fluoride (PVDF) piezoelectric polymers and inorganic  $0.5\text{Ba}(\text{Zr}_{0.2}\text{Ti}_{0.8})\text{O}_3$ - $0.5(\text{Ba}_{0.7}\text{Ca}_{0.3})\text{TiO}_3$  (BZT-BCT) NWs, which exhibited high voltage coefficients<sup>[74]</sup>. Prior to the preparation of ultrasonically-excited piezoelectric thin-film nanogenerators, the researchers applied polydopamine (PDA) coatings on the surface of BZT-BCT NWs to enhance the interfacial bonding between the NWs and the PVDF polymer. The developed PVDF/BZT-BCT@PDA thin-film nanogenerators, with a thickness of approximately  $10 \text{ }\mu\text{m}$ , as depicted in Figure 8B, successfully achieved ultrasound-driven ES of the rat sciatic nerve.

Piezoelectric polymers are a promising candidate for neurostimulators due to their ability to align with soft organic tissues. Das *et al.* developed a biodegradable and biocompatible piezoelectric nanofiber scaffold using PLLA, which provides a programmable surface charge to promote bone development<sup>[75]</sup>. Chen *et al.*



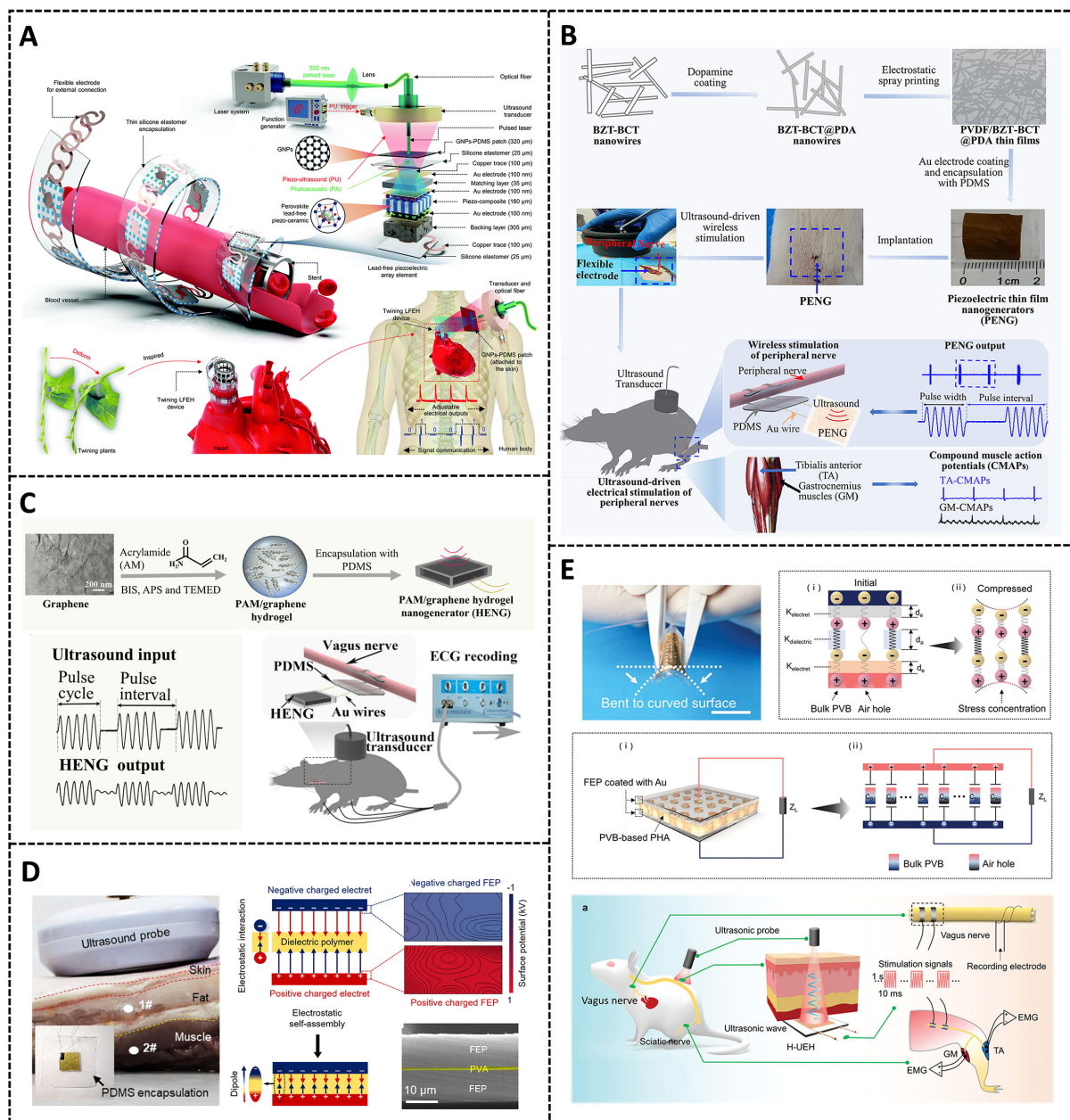


**Figure 8.** (A) 3D-wrapped wirelessly implantable ultrasound-driven electrical stimulation system based on PA and PU technologies<sup>[73]</sup>. Reprinted with permission. Copyright 2021, Rsc Publishing; (B) PVDF/BZT-BCT@PDA thin-film nanogenerator for nerve stimulation<sup>[74]</sup>. Reprinted with permission. Copyright 2021, Elsevier; (C) HENG-based vagus nerve stimulator<sup>[76]</sup>. Reprinted with permission. Copyright 2021, Elsevier; (D) Ultrathin piezoelectret with sandwiched polymer structure with good implantability<sup>[77]</sup>. Reprinted with permission. Copyright 2021, Elsevier; (E) H-UEH is based on multilayered piezoelectric electret based on air-hole arrays for nerve stimulation<sup>[78]</sup>. Reprinted with permission. Copyright 2022, John Wiley and Sons. BZT-BCT:  $0.5\text{Ba}(\text{Zr}_{0.2}\text{Ti}_{0.8})\text{O}_3-0.5(\text{Ba}_{0.7}\text{Ca}_{0.3})\text{TiO}_3$ ; ECG: electrocardiography; FEP: fluorinated ethylene propylene; HENG: high-performance hydrogel nanogenerators; H-UEH: high-efficiency ultrasonic energy harvester; PA: photoacoustic; PDMS: polydimethylsiloxane; PDA: polydopamine; PU: piezo-ultrasound; PVA: poly(vinyl alcohol); PVDF: polyvinylidene fluoride.

proposed a wireless rechargeable, battery-free vagus nerve stimulator based on high-performance hydrogel nanogenerators (HENG) implanted in the body [Figure 8C]<sup>[76]</sup>. HENG is a liquid-based nanogenerator that integrates graphene into the polyacrylamide (PAM) hydrogel matrix. By modulating compressive force, the double electric layer at the PAM/electrolyte interface induces ACs through electrostatic induction, thereby

providing ES to the vagus nerve. This stimulation effectively suppresses pro-inflammatory cytokines. With dimensions of 1.5 cm × 1.5 cm × 1 mm and an ultrasound power of 0.3 W/cm<sup>2</sup>, the HENG generated a short-circuit current of 1.6 mA, which is comparable to the output current of commercial neurostimulators.

Piezoelectric electrets extend the piezoelectric effect to non-polar polymers, in contrast to current piezoelectric materials. They possess a high equivalent piezoelectric coefficient, exceptional flexibility, and excellent biocompatibility. In [Figure 8D](#), Xu *et al.* presented an ultrathin piezoelectric electret with a sandwich polymer structure, which achieved piezoelectric constants ( $d_{33}$ ) up to 930 pC·N<sup>-1</sup> through electrostatic interactions<sup>[77]</sup>. The piezoelectret utilizes a polyvinyl butyral (PVB) dielectric with a large modulus of elasticity. It has good implantability. In [Figure 8E](#), Wan *et al.* demonstrated an ultrathin multilayered piezoelectric electret (~75 μm) with strong piezoelectric properties<sup>[78]</sup>. They achieved this by introducing an array of air holes connected in parallel in the dielectric layer between a pair of piezoelectric electrodes, which allows for greater strain from stronger stress concentration, enabling efficient ultrasound energy harvesting. It achieves a peak output power of about 13.13 mW and a short-circuit current of about 2.2 mA at an ultrasound excitation of 25 mW/cm<sup>2</sup>. A series of peripheral nerve stimulations, including sciatic and vagus nerves, were successfully performed in a rat model, demonstrating the broader range of potential applications for piezoelectric electret-based implantable neurostimulators.

## OTHER FORMS OF NERVE STIMULATION

Traditional ES achieves continuous wired power supply through implantation, but this approach can lead to severe foreign body reactions, negatively affecting animal movement and causing other adverse effects. Additionally, non-specific ES poses challenges in accurately targeting the desired tissue, often resulting in neurological complications. Consequently, numerous novel neural stimulation methods have been developed to address these challenges and mitigate the adverse effects associated with ES. This section provides a description of flexible devices utilized in various innovative nerve stimulation methods, including magnetism, light, and ultrasound. Furthermore, the developmental trends of these devices are highlighted.

### Magnetic stimulation

Unlike ES, MS does not deliver current through electrodes but rather applies current stimulation through EM induction. The MS stimulator delivers a short-lasting current through the coil that produces a strong time-varying EM field perpendicular to the transducer coil. The magnetic field passes directly through the tissue surrounding the brain and induces a phasic electric field in the target tissue. An action potential is triggered when the electric field induced by the MS is strong enough to depolarize the membrane potential of a given neuron above a certain threshold.

#### *Transcranial magnetic stimulation*

Wireless modulation of neural activity is clinically accessible through transcranial magnetic stimulation (TMS), which does not require an implanted device<sup>[79,80]</sup>. Magnetic fields generated by coils placed on the scalp can effectively penetrate the electrically insulated skull, allowing MS to induce strong, moderately spatially focused intracranial currents in brain tissue. Depending on the stimulation site, sequence parameters, and other factors, TMS pulses can lead to long-term changes that either enhance or inhibit neuronal excitability and specific behaviors.

It is important to note that TMS primarily modulates the cerebral cortex<sup>[81]</sup> and has limitations in terms of depth-focused regions<sup>[82,83]</sup>, making DBS with TMS currently unfeasible. TMS can be used for various neuronal stimulation by adjusting different stimulation parameters. Single-pulse TMS (spTMS)<sup>[84]</sup> and paired-pulse TMS (ppTMS)<sup>[85]</sup> can target time-dependent neuronal processes, with their effects lasting only



a fraction of a second. In contrast, longer sequences of repetitive TMS pulses (rTMS) can induce lasting neuroplastic changes, offering therapeutic potential. Therefore, TMS pulses are typically administered in sequences<sup>[86,87]</sup> or in more complex patterns, such as theta pulse stimulation (TBS<sup>[88]</sup>), quad pulse stimulation (QPS<sup>[89]</sup>), and repetitive ppTMS (rppTMS<sup>[90]</sup>). In general, high-frequency rTMS (5-25 Hz) tends to be facilitative<sup>[86]</sup>, while low-frequency rTMS (~1 Hz) typically reduces excitability<sup>[87]</sup>. However, it is important to note that the mechanisms underlying TMS activation and rTMS-induced plasticity are intricate and not fully understood.

#### *Micromagnetic stimulation*

TMS devices are typically large and are less effective for reaching deeper subcortical brain targets. However, studies have found that sub-millimeter coils can effectively activate neural tissue, and the orientation of these coils relative to neural tissue can yield specific neural responses. These findings underscore the feasibility of neurostimulation using miniature magnetic coils, small enough to be implanted within the brain parenchyma. As a result, micromagnetic stimulation ( $\mu$ MS) emerges as a viable alternative to traditional TMS devices. One advantage of  $\mu$ MS is its potential compatibility with MRI when turned off. This is because the  $\mu$ MS coil is electrically isolated from adjacent tissue, thereby limiting the extent of thermal induction. Furthermore, micro-coils can be placed in close proximity to target tissues, potentially enhancing the precision of elicited neural activity. These coils can also be encapsulated with various biocompatible materials.

For instance, when microcoils were used to stimulate rabbit retinal ganglion cells, it was observed that  $\mu$ MS induced neural activity<sup>[11]</sup> [Figure 9A]. Subsequently,  $\mu$ MS was shown to activate neural circuits at the systemic level and was applied to the dorsal nucleus of the cochlea to activate hypothalamic neurons [Figure 9B]. Importantly, different MS parameters were found to yield varying efficacy and characteristics<sup>[91]</sup>. Furthermore, the development of miniature solenoids, with dimensions as small as 80  $\mu$ m by 40  $\mu$ m and featuring a magnetic core to generate a stronger magnetic field, represents a significant advancement. These solenoids are fully encapsulated in biocompatible coatings. The reduction in the size of  $\mu$ MS probes results in improved spatial resolution, reduced heat generation by the inductor, and the ability to activate more neurons around the probe. As illustrated in Figure 9C, these solenoids are compact enough to be implanted within the brain and used as chronic neural interfaces. They have demonstrated their effectiveness as alternatives to existing electrode-based stimulation devices<sup>[92]</sup>.

### **Optic stimulation**

#### *Optogenetics*

The rapid advancement of optogenetic modulation, a distinct form of brain stimulation, along with its adaptable devices, is noteworthy. Optogenetics serves as the fundamental basis for optogenetic technologies. In the 1960s, scholars initially proposed the conversion of electrical information from neurons into visible light signals. When neurons generate electrical impulses, the electric field alters the molecular structure of the chemical dyes used for neuronal staining, resulting in a change in color. These chemical dyes specifically adhere to the neuron membrane's surface and do not penetrate the cell. Measuring the color of the dye allows for the visualization of neural tissue, facilitating a clear observation of brain activity. Building upon this line of inquiry, scholars conducted further investigations. In 2005, Boyden *et al.* successfully expressed light-sensitive proteins in mammalian neurons by combining lentiviral gene delivery with high-speed light switches to transfect a naturally occurring algal protein called channelrhodopsin-2 (ChR-2). Through the regulation of neurons using various light wavelengths, they gained control over action potentials between neurons and the excitatory/inhibitory transmission among synapses, thereby paving the way for optogenetic technology<sup>[93]</sup>.

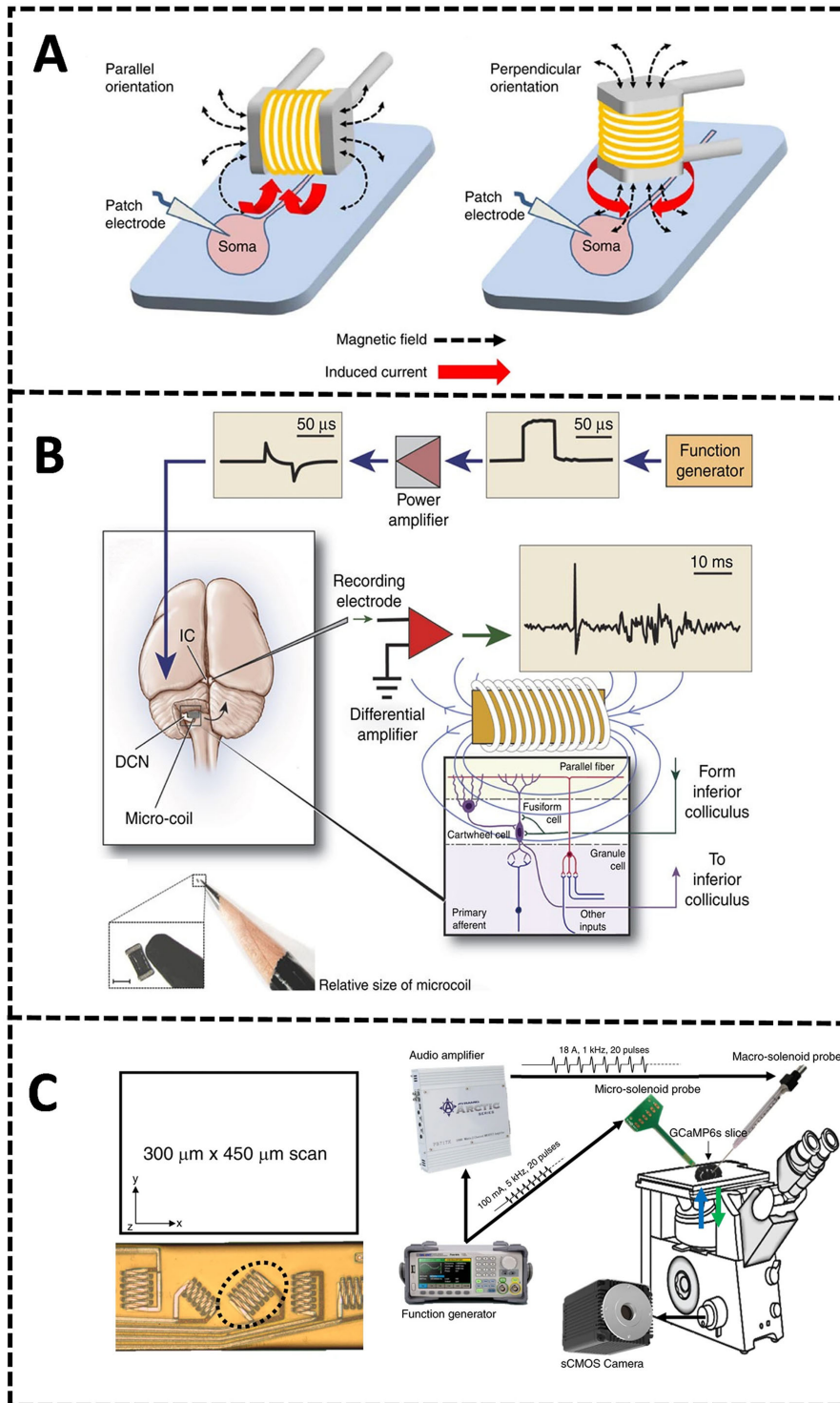


**Figure 9.** (A) Microcoil used to stimulate rabbit retinal ganglion cells<sup>[11]</sup>. Reprinted with permission. Copyright 2012, Springer Nature; (B) Microcoil used to stimulate the cochlear dorsal nucleus to activate hypothalamic neurons<sup>[91]</sup>. Copyright 2013, Springer Nature; (C) Miniature solenoidal micromagnetic stimulator used for brain slicing<sup>[92]</sup>. Copyright 2021, Springer Nature. DCN: Dorsal cochlear nucleus; IC: inferior colliculus.

The principle of optogenetics involves employing gene manipulation techniques to introduce light-sensitive genes (such as ChR-2) into neurons, enabling the production of specialized ion channels. Upon exposure to

different light wavelengths, these ion channels selectively facilitate the passage of cations or anions, resulting in alterations in the membrane potential on both sides of the cell membrane. This process serves the purpose of selectively stimulating or inhibiting cells. Optogenetics, a technique that combines genetic engineering with light manipulation, is currently undergoing refinement and finding extensive applications in various domains, particularly in the investigation of brain circuit function.

In 2021, Yang *et al.* published a study on an implantable wireless optogenetic electronic device, highlighting its promising potential for conducting optogenetic experiments on individual and group animal behavior<sup>[94]</sup>. The study involved the development of both head-mounted (HM) and back-mounted (BM) flexible wireless implanted devices [Figure 10A]. The researchers utilized  $\mu$ -ILEDs, which were fixed at the tip of the puncture probe, to deliver optical stimulation to neurons. These  $\mu$ -ILEDs were integrated with near-field communication and microprocessor technology, enabling real-time control of the optical stimulation. The devices were powered through magnetic inductive coupling, while the incorporation of mechanically designed extendable flexible electrical technology ensures the long-term stability of the implanted device and substantially reduces the harm inflicted on animals during the implantation process. Furthermore, the researchers developed an NFC-programmable system based on the device, which allows real-time control of interbrain dynamics in investigations involving multiple brains. Moreover, it facilitates optogenetic studies on group behavior.

Rajalingham *et al.* from MIT utilized optogenetics to investigate non-human primate behavior through the development of Opto-Array [Figure 10B]. The long-term implantation of the flexible light-emitting diode array enables high-throughput optogenetic interventions and facilitates the study of behavior-related optogenetics in intricate brains, including those of rhesus monkeys<sup>[95]</sup>. This investigation ruled out any interference from photothermal effects and provided evidence that optogenetics based on Opto-Array can modify the primary visual cortex of macaques, resulting in significant changes in brightness discrimination. This finding indicates that Opto-Array's reliable technical support can be leveraged for optogenetic research in complex brain behaviors, among other areas.

#### *Infrared light neurostimulation*

The safety of optogenetics remains uncertain due to its reliance on viral gene transfection. The application of optogenetics in disease treatment is limited and challenging, particularly regarding its integration with flexible devices. In 2005, Wells *et al.* introduced a groundbreaking approach to neural stimulation by utilizing pulsed infrared laser irradiation at levels significantly below the tissue damage threshold<sup>[96]</sup>. With ongoing improvements in biological mechanisms and device fabrication processes, the techniques for modulating neuronal function through direct optical stimulation are advancing as well.

Nowadays, there is a widely accepted understanding that infrared neural stimulation operates through a photothermal mechanism, wherein the absorption of infrared light by water generates heat. This sudden temperature change produces transmembrane capacitive currents or activates thermosensitive ion channels, which, in turn, affects the electrical activity of neurons. Nevertheless, excessive photothermal effects can frequently lead to cellular and tissue damage. An alternative hypothesis suggests that the generation of action potentials through infrared neural stimulation relies on the activity of ion channel proteins located on the cell membrane, with the vibrational frequency of chemical bonds within proteins aligning with the mid-infrared range. In the event that mid-infrared light of a specific frequency resonates with crucial chemical bonds within ion channels, it has the potential to modulate channel function and consequently impact neuronal electrical activity.

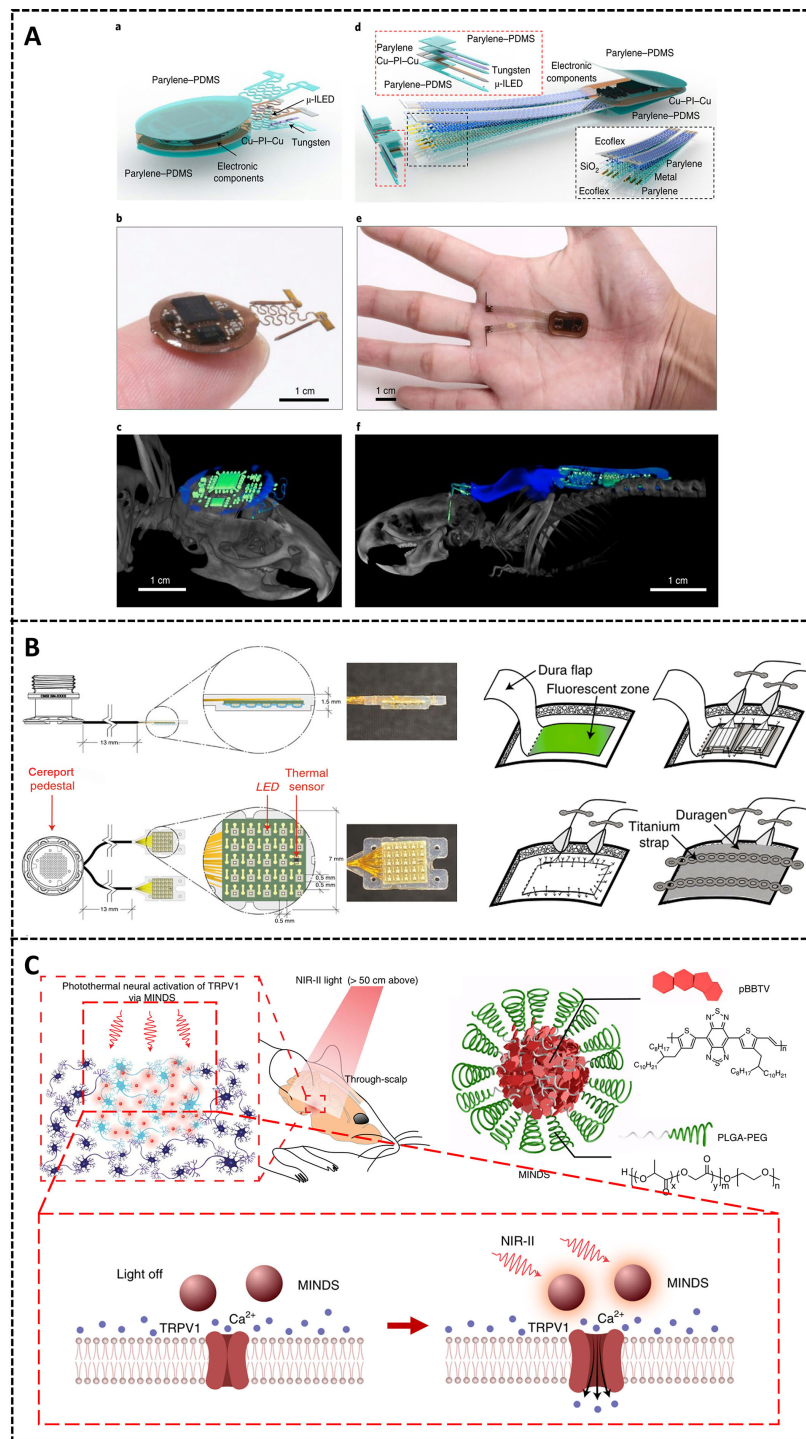


**Figure 10.** Flexible optical stimulation devices. (A) Schematic diagram of HM and BM flexible wireless devices, which are used for optogenetic research on unrestrained animals and have dynamically programmable operations<sup>[94]</sup>. Reprinted with permission. Copyright 2021, Springer Nature; (B) Schematic diagram of the Opto-Array array design<sup>[95]</sup>. Reprinted with permission. Copyright 2021, Springer Nature; (C) Infrared light stimulation flexible device - MINDS for penetrative neural regulation under NIR-II. MINDS is composed of a pBBTV conjugated copolymer core (red hexagons) and a PLGA-PEG polymer shell (green spirals)<sup>[97]</sup>. Reprinted with permission. Copyright 2022, Springer Nature. BM: Back-mounted; HM: head-mounted; MINDS: macromolecular infrared nanotransducers; NIR-II: near-infrared pulsed light; pBBTV: poly(benzobisthiadiazole-alt-vinylene); PDMS: polydimethylsiloxane; PLGA-PEG: poly(lactic-co-glycolic acid)-polyethylene glycol; TRPV1: transient receptor potential cation channel subfamily V member 1.



In 2022, Wu *et al.* presented a novel technology for deep brain neural regulation using near-infrared light capable of penetrating the intact scalp and skull<sup>[97]</sup>. This technology, depicted in [Figure 10C](#) and based on macromolecular infrared nanotransducers (MINDS), utilizes near-infrared pulsed light (NIR-II) to elicit DBS in awake and freely behaving mice. Comprising pBBTV and poly(lactic-co-glycolic acid)-polyethylene glycol (PLGA-PEG), MINDS possesses an average diameter of around 40 nm. The pBBTV core demonstrates efficient absorption of 1,064 nm near-infrared light, converting it into heat, whereas the PLGA-PEG shell exhibits favorable water solubility and biocompatibility. Experimental tests revealed that MINDS achieves a photothermal conversion efficiency of 71% at 1,064 nm, maintaining structural stability under normal physiological conditions and exhibiting exceptional photostability during repeated NIR-II irradiation. Subsequent to the injection of MINDS into the mouse brain, the *in vivo* verification of NIR-II neural stimulation was conducted in the mouse hippocampus and motor cortex. The local thermal effect induced by MINDS activates the heat channel protein TRPV1, selectively modulating the activity of neurons that express TRPV1 in the deep brain of mice. This study presents a novel approach to neural regulation in sociobehavioral investigations, circumventing physical constraints and potential brain tissue damage associated with invasive equipment, in contrast to conventional optical neural stimulation methods.

### Ultrasonic stimulation

Since 1929, researchers have been observing the fascinating effects of ultrasound on neural activity<sup>[98]</sup>. In recent years, the numerous advantages and potential of ultrasound nerve stimulation have come into sharper focus. Studies have shown that by using focused ultrasound, it is possible to influence sensory and motor responses in different animals, such as rodents<sup>[99,100]</sup>, larger animals<sup>[101,102]</sup>, and primates<sup>[103-105]</sup>. Surprisingly, ultrasound has the remarkable capacity to pass through the skull, allowing for long-distance transmission. It reaches deep brain neuromodulation without physically or thermally damaging the delicate tissue network by modifying the electrophysiological activity of the neurons in the stimulation area based on mechanical effect<sup>[106,107]</sup> and the phenomenon of non-inertial cavitation<sup>[108]</sup>. Mechanical effect means that low-intensity focused ultrasound can cause mechanical vibration of the cell membrane of the nerve cells, stretching the phospholipid bilayer and exerting mechanical force on the cell membrane. It is worth noting that the cell membrane contains a vast number of highly sensitive to mechanical force ion channels. Applying low-intensity focused ultrasound will unavoidably cause these ion channels to open or close, thereby altering the electrophysiological activity of the stimulated nerve cells and achieving neurostimulation. Cavitation is the phenomenon in which small liquid bubbles vibrate, expand, and collapse due to modifications in stress within the acoustic field resulting from ultrasonic stretching and compression oscillations. Two types of ultrasonic cavitation exist: stable and inertial cavitation. In the non-inertial cavitation process, low-intensity ultrasound bubbles focus and oscillate repetitively between the phospholipid bilayers of the cell membrane, instigating localized shear stresses which, in turn, trigger force-sensitive ion channels residing in the cell membrane and produce neural stimulation. One may successfully alter the course of neuromodulatory consequences, giving them a greater sense of significance, by deftly adjusting factors such as the center frequency and strength of ultrasonic pulses<sup>[109-112]</sup>.

Researchers have extensively studied miniaturized ultrasound neurostimulation devices based on an initial understanding of the principle mechanisms of ultrasound neuromodulation. Our group reported the specifications of a small, focused ultrasound transducer, as depicted in [Figure 11A](#), which had a center frequency of 650 kHz, a diameter of 12 mm, a focal point of 9 mm, and a peak acoustic pressure of up to 0.47 MPa in the focal area<sup>[113]</sup>. Kook *et al.* developed a lightweight miniature ultrasound neuromodulation system, weighing just 0.75 g, through the integration of a 3D-printed acoustic lens and a MEMS ultrasound transducer [[Figure 11B](#)]<sup>[114]</sup>. This system enables numerical analysis and design of neural stimulation based on the frequency and pressure of transmitted ultrasound beams, allowing for precise stimulation of multiple target areas through acoustic holography. The above-mentioned findings demonstrate that ultrasonic modulation provides a safe and non-invasive method for stimulating the nervous system.

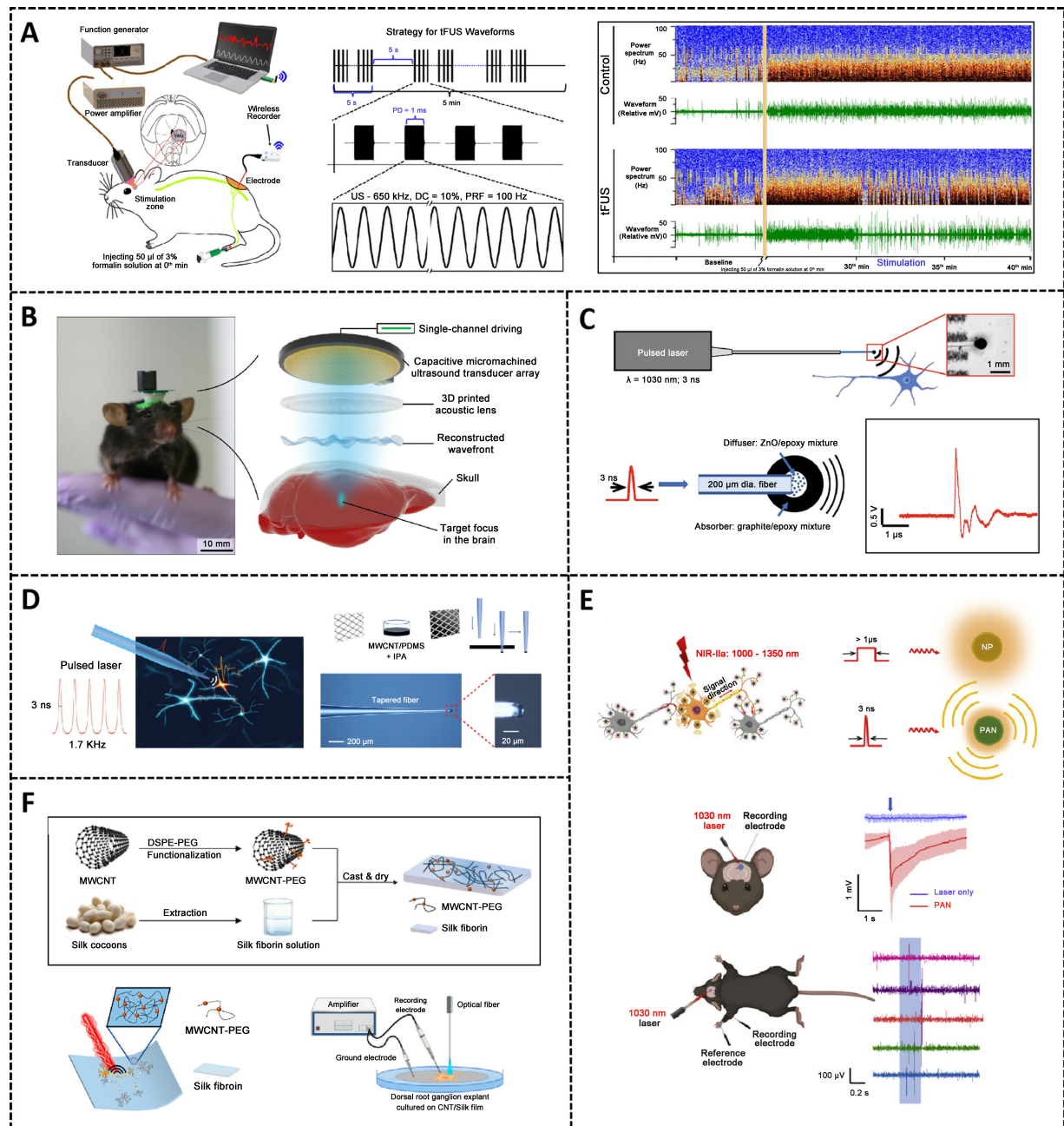


**Figure 11.** Ultrasound neurostimulators. (A) Miniatured focused ultrasound transducer to stimulate PAG for analgesia<sup>[113]</sup>. Reprinted with permission. Copyright 2016, Springer Nature; (B) Ultralight miniaturized focused ultrasound brain stimulation system with multi-region targeting capability<sup>[114]</sup>. Reprinted with permission. Copyright 2023, Springer Nature; (C) Miniaturized FOC for neural activation<sup>[115]</sup>. Reprinted with permission. Copyright 2020, Springer Nature; (D) TFOE for neuromodulation of individual neurons or subcellular structures<sup>[116]</sup>. Reprinted with permission. Copyright 2021, Springer Nature; (E) Photoacoustic nanotransducer injected into the brain to achieve neurostimulation<sup>[113]</sup>. Reprinted with permission. Copyright 2020, Elsevier; (F) Nanocomposite protein scaffolds to promote nerve growth<sup>[117]</sup>. Reprinted with permission. Copyright 2022, American Chemical Society. FOC: Fiber-Optoacoustic Converter; IPA: isopropyl alcohol; MWCNT: multi-walled carbon nanotubes; PAG: periaqueductal gray; PDMS: polydimethylsiloxane; TFOE: tapered fiber optoacoustic emitter.



The intricate electrical connections in piezoelectric or capacitive ultrasound transducers impede device miniaturization and hinder their use in wearable or implantable neuromodulation applications. However, the inadequate frequency characteristics of piezoelectric ultrasound result in a spatial resolution of only a few millimeters, which fails to meet the demands for precise spatial neural stimulation. Researchers have explored the use of the photoacoustic effect to generate acoustic waves for direct neuromodulation of brain nerves. Jiang *et al.* developed a miniaturized Fiber-Optoacoustic Converter (FOC) that achieved stable neural activation within a 500  $\mu\text{m}$  radius of the fiber optic tip [Figure 11C]<sup>[115]</sup>. The electrophysiological recordings exhibited a reflection latency of < 100 ms, enabling precise modulation of the motor and somatosensory cortex in mice with sub-millimeter spatial accuracy. In comparison to the piezoelectric-focused ultrasound stimulator, the photoacoustic stimulator, with a tip diameter of approximately 600  $\mu\text{m}$ , generates low peak sound pressure, preventing the occurrence of thermal effects in biological tissues and enhancing its implantability. Building upon this foundation, Shi *et al.* introduced a tapered fiber optoacoustic emitter (TFOE) capable of generating sub-millisecond ultrasound pulses with a spatial accuracy of up to 39.6  $\mu\text{m}$ , facilitating precise modulation of individual neurons or subcellular structures such as axons or dendrites<sup>[116]</sup> [Figure 11D]. Photoacoustic transducers have demonstrated sub-millimeter level *ex vivo* and *in vivo* neurostimulation capabilities in this field and hold promise as an emerging therapeutic tool for neurodegenerative diseases in the future.

Typical ultrasound modulation devices primarily comprise an ultrasound stimulator and an external unit, connected mainly through a wired interface. However, conventional power supply methods for implantable or wearable devices are constrained by inherent limitations in size, capacity, and lifespan, hindering their practical implementation. Researchers have integrated biocompatible nanomaterials with photoacoustic transducers to develop implantable nano-ultrasound stimulation devices capable of wireless ultrasound generation through the supply of energy via highly penetrative laser radiation. Jiang *et al.* developed biocompatible and biodegradable photoacoustic nanotransducers (PANs) using semiconducting polymer nanoparticles [Figure 11E]<sup>[113]</sup>. Injection of PANs into the cerebral cortex enables non-genetic neural activation of neurons *in vitro* and the motor cortex in the mouse brain. The PANs achieved precise activation of individual neurons when excited by NIR-II light transmitted through a tapered optical fiber. Zheng *et al.* employed a nanocomposite technique to incorporate CNTs into silk fibroin, yielding a flexible and biocompatible photoacoustic material [Figure 11F]<sup>[117]</sup>. Implantation of these CNT/silk scaffolds in the target region enables neurostimulation and nerve development, facilitated by the application of NIR-II light with significant penetration depth. The stimulation provided by these NWs presents a novel approach to ultrasound.

## CONCLUSION AND OUTLOOK

With the continuous advancement of neurostimulation devices, neurostimulation has emerged as a crucial approach for treating neurological diseases. This review presents flexible devices with diverse stimulation modes that have demonstrated outstanding performance and therapeutic potential. However, significant challenges remain to be addressed, and the following aspects warrant further attention in future development.

(1) High biocompatibility: while most neurostimulation devices are invasive and may damage biological tissue upon contact, the use of polymer materials with improved biocompatibility as flexible substrates or electrodes is common. However, their Young's modulus still lags significantly behind that of biological tissues. Therefore, the selection of more flexible and thinner materials is necessary to manufacture devices capable of achieving unprecedented effects.

(2) Long-term stability: certain neurological diseases are chronic in nature and necessitate implants for long-term neurostimulation within the body. The presence of the device in the body's biological environment accelerates device aging and failure, potentially causing harm to the patient. Managing chronic conditions necessitates the use of long-lasting, flexible electronic devices capable of maintaining stable functionality during human activities and within biological environments.

(3) Wireless and low power consumption: wireless connections between implantable devices and signal-emitting devices can minimize invasiveness and eliminate the risks associated with repeated surgeries. Powering the device using energy from motion or external energy transmission (e.g., magnetism, ultrasound) significantly reduces the risk of battery depletion in implantable electronic devices, obviating the need for additional external power sources. Consequently, the development of neurostimulation devices should prioritize wireless functionality and low power consumption.

(4) Achieve closed-loop stimulation: closed-loop stimulation enables accurate detection of specific nerve signals for precise delivery of treatment. For instance, the predominant stimulation mode in most DBS techniques is open-loop stimulation, which administers fixed-pulse ES based on predetermined parameters. In comparison, closed-loop stimulation offers greater precision and efficacy. The integration of neurostimulation devices with neural signal recording devices represents a crucial advancement for enhancing therapeutic outcomes.

The future development of flexible devices for nerve stimulation hinges on continuous innovation in materials, design, and manufacturing technology. We firmly believe that through collaboration among ICs, neuroscience, clinical medicine, and other disciplines, flexible devices for nerve stimulation will assume a pivotal role in medical applications.

## **DECLARATIONS**

### **Authors' contributions**

Wrote the original draft: Liu ZQ, Yu XY, Huang J, Wu XY

Supervised, reviewed, and revised the manuscript: Zhu BP, Wang ZY

### **Availability of data and materials**

Not applicable.

### **Financial support and sponsorship**

This work is financially supported by the National Natural Science Foundation of China (No. U22A20259) and Shenzhen Basic Science Research (grant NOs. JCYJ20200109110006136, JCYJ20220530160602006).

### **Conflicts of interest**

All authors declared that there are no conflicts of interest.

### **Ethical approval and consent to participate**

Not applicable.

### **Consent for publication**

Not applicable.

## Copyright

© The Author(s) 2024.

## REFERENCES

1. Woods GA, Rommelfanger NJ, Hong G. Bioinspired materials for *in vivo* bioelectronic neural interfaces. *Matter* 2020;3:1087-113. DOI PubMed PMC
2. Song E, Li J, Rogers JA. Barrier materials for flexible bioelectronic implants with chronic stability - current approaches and future directions. *APL Mater* 2019;7:050902. DOI
3. Song E, Li J, Won SM, Bai W, Rogers JA. Materials for flexible bioelectronic systems as chronic neural interfaces. *Nat Mater* 2020;19:590-603. DOI PubMed
4. Kim DH, Viventi J, Amsden JJ, et al. Dissolvable films of silk fibroin for ultrathin conformal bio-integrated electronics. *Nature Mater* 2010;9:511-7. DOI PubMed PMC
5. Ressler KJ, Mayberg HS. Targeting abnormal neural circuits in mood and anxiety disorders: from the laboratory to the clinic. *Nat Neurosci* 2007;10:1116-24. DOI PubMed PMC
6. Wells JD, Kao C, Jansen ED, Konrad PE, Mahadevan-Jansen A. Application of infrared light for *in vivo* neural stimulation. *J Biomed Opt* 2005;10:064003. DOI PubMed
7. Legon W, Sato TF, Opitz A, et al. Transcranial focused ultrasound modulates the activity of primary somatosensory cortex in humans. *Nat Neurosci* 2014;17:322-9. DOI
8. Liang L, Liu C, Cai P, et al. Highly specific differentiation of MSCs into neurons directed by local electrical stimuli triggered wirelessly by electromagnetic induction nanogenerator. *Nano Energy* 2022;100:107483. DOI
9. Palanker D, Vankov A, Huie P, Baccus S. Design of a high-resolution optoelectronic retinal prosthesis. *J Neural Eng* 2005;2:S105-20. DOI PubMed
10. Zhang T, Liang H, Wang Z, et al. Piezoelectric ultrasound energy - harvesting device for deep brain stimulation and analgesia applications. *Sci Adv* 2022;8:eabk0159. DOI PubMed PMC
11. Bonmassar G, Lee SW, Freeman DK, Polasek M, Fried SI, Gale JT. Microscopic magnetic stimulation of neural tissue. *Nat Commun* 2012;3:921. DOI PubMed PMC
12. Rand D, Jakešová M, Lubin G, et al. Direct electrical neurostimulation with organic pigment photocapacitors. *Adv Mater* 2018;30:1707292. DOI PubMed
13. Jiang Y, Huang Y, Luo X, et al. Neural stimulation *in vitro* and *in vivo* by photoacoustic nanotransducers. *Matter* 2021;4:654-74. DOI
14. Cogan SF. Neural stimulation and recording electrodes. *Annu Rev Biomed Eng* 2008;10:275-309. DOI PubMed
15. Schwab JM, Hamani C. The history and future of deep brain stimulation. *Neurotherapeutics* 2008;5:3-13. DOI PubMed PMC
16. Kellaway P. The part played by electric fish in the early history of bioelectricity and electrotherapy. *Bull Hist Med* 1946;20:112-137. PubMed
17. Sackeim HA. Modern electroconvulsive therapy: vastly improved yet greatly underused. *JAMA Psychiatry* 2017;74:779-80. DOI PubMed
18. Benabid AL, Pollak P, Louveau A, Henry S, de Rougemont J. Combined (thalamotomy and stimulation) stereotactic surgery of the VIM thalamic nucleus for bilateral parkinson disease. *Stereotact Funct Neurosurg* 1987;50:344-6. DOI
19. Chen XL, Xiong YY, Xu GL, Liu XF. Deep brain stimulation. *Intervent Neurol* 2013;1:200-12. DOI PubMed PMC
20. Elkin BS, Ilankovan A, Morrison B III. Age-dependent regional mechanical properties of the rat hippocampus and cortex. *J Biomech Eng* 2010;132:011010. DOI PubMed
21. Wu X, Peng H. Polymer-based flexible bioelectronics. *Sci Bull* 2019;64:634-40. DOI
22. Lai HY, Liao LD, Lin CT, et al. Design, simulation and experimental validation of a novel flexible neural probe for deep brain stimulation and multichannel recording. *J Neural Eng* 2012;9:036001. DOI
23. Wurth S, Capogrosso M, Raspopovic S, et al. Long-term usability and bio-integration of polyimide-based intra-neural stimulating electrodes. *Biomaterials* 2017;122:114-29. DOI
24. Fujie T, Ahadian S, Liu H, et al. Engineered nanomembranes for directing cellular organization toward flexible biodevices. *Nano Lett* 2013;13:3185-92. DOI
25. Xiang Z, Yen S, Xue N, et al. Ultra-thin flexible polyimide neural probe embedded in a dissolvable maltose-coated microneedle. *J Micromech Microeng* 2014;24:065015. DOI
26. Minev IR, Musienko P, Hirsch A, et al. Electronic dura mater for long-term multimodal neural interfaces. *Science* 2015;347:159-63. DOI
27. Zhu M, Wang H, Li S, et al. Flexible electrodes for *in vivo* and *in vitro* electrophysiological signal recording. *Adv Healthc Mater* 2021;10:2100646. DOI PubMed
28. David-Pur M, Bareket-Keren L, Beit-Yaakov G, Raz-Prag D, Hanein Y. All-carbon-nanotube flexible multi-electrode array for neuronal recording and stimulation. *Biomed Microdevices* 2014;16:43-53. DOI PubMed PMC
29. Vitale F, Summerson SR, Aazhang B, Kemere C, Pasquali M. Neural stimulation and recording with bidirectional, soft carbon nanotube fiber microelectrodes. *ACS Nano* 2015;9:4465-74. DOI PubMed

30. McCallum GA, Sui X, Qiu C, et al. Chronic interfacing with the autonomic nervous system using carbon nanotube (CNT) yarn electrodes. *Sci Rep* 2017;7:11723. DOI PubMed PMC
31. Tang R, Zhang C, Liu B, et al. Towards an artificial peripheral nerve: liquid metal-based fluidic cuff electrodes for long-term nerve stimulation and recording. *Biosens Bioelectron* 2022;216:114600. DOI
32. Fan X, Chen Z, Sun H, Zeng S, Liu R, Tian Y. Polyelectrolyte-based conductive hydrogels: from theory to applications. *Soft Sci* 2022;2:10. DOI
33. Cong Y, Fu J. Hydrogel - tissue interface interactions for implantable flexible bioelectronics. *Langmuir* 2022;38:11503-13. DOI PubMed
34. Kim SD, Park K, Lee S, et al. Injectable and tissue-conformable conductive hydrogel for MRI-compatible brain-interfacing electrodes. *Soft Sci* 2023;3:18. DOI
35. Zhang J, Wang L, Xue Y, et al. Engineering electrodes with robust conducting hydrogel coating for neural recording and modulation. *Adv Mater* 2023;35:2209324. DOI
36. Nguyen TK, Barton M, Ashok A, et al. Wide bandgap semiconductor nanomembranes as a long-term biointerface for flexible, implanted neuromodulator. *Proc Natl Acad Sci U S A* 2022;119:e2203287119. DOI PubMed PMC
37. Lin JC. A new IEEE standard for safety levels with respect to human exposure to radio-frequency radiation. *IEEE Antennas Propag Mag* 2006;48:157-9. DOI
38. Fotopoulou K, Flynn BW. Wireless power transfer in loosely coupled links: coil misalignment model. *IEEE Trans Magn* 2011;47:416-30. DOI
39. Freeman DK, O'Brien JM, Kumar P, et al. A sub-millimeter, inductively powered neural stimulator. *Front Neurosci* 2017;11:659. DOI PubMed PMC
40. Maeng LY, Murillo MF, Mu M, et al. Behavioral validation of a wireless low-power neurostimulation technology in a conditioned place preference task. *J Neural Eng* 2019;16:026022. DOI PubMed PMC
41. Singer A, Dutta S, Lewis E, et al. Magnetolectric materials for miniature, wireless neural stimulation at therapeutic frequencies. *Neuron* 2020;107:631-43.e5. DOI PubMed PMC
42. Yu Z, Chen JC, Alrashdan FT, et al. MagnI: a magnetolectrically powered and controlled wireless neurostimulating implant. *IEEE Trans Biomed Circuits Syst* 2020;14:1241-52. DOI PubMed PMC
43. Chen JC, Kan P, Yu Z, et al. A wireless millimetric magnetolectric implant for the endovascular stimulation of peripheral nerves. *Nat Biomed Eng* 2022;6:706-16. DOI PubMed PMC
44. Guduru R, Liang P, Hong J, et al. Magnetolectric 'spin' on stimulating the brain. *Nanomedicine* 2015;10:2051-61. DOI PubMed PMC
45. Kozielski KL, Jahanshahi A, Gilbert HB, et al. Nonresonant powering of injectable nanoelectrodes enables wireless deep brain stimulation in freely moving mice. *Sci Adv* 2021;7:eabc4189. DOI PubMed PMC
46. Han F, Ma X, Zhai Y, et al. Strategy for designing a cell scaffold to enable wireless electrical stimulation for enhanced neuronal differentiation of stem cells. *Adv Healthc Mater* 2021;10:2100027. DOI
47. Tang B, Zhuang J, Wang L, et al. Harnessing cell dynamic responses on magnetolectric nanocomposite films to promote osteogenic differentiation. *ACS Appl Mater Interfaces* 2018;10:7841-51. DOI
48. Zhang Y, Chen S, Xiao Z, et al. Magnetolectric nanoparticles incorporated biomimetic matrix for wireless electrical stimulation and nerve regeneration. *Adv Healthc Mater* 2021;10:2100695. DOI
49. Qi F, Gao X, Shuai Y, et al. Magnetic-driven wireless electrical stimulation in a scaffold. *Compos B Eng* 2022;237:109864. DOI
50. Goetz G, Palanker D, Cizmar T. Holographic display system for photovoltaic retinal prosthesis. *Invest Ophthalmol Vis Sci* 2013;54:352. Available from: <https://iovs.arvojournals.org/article.aspx?articleid=2148311>. [Last accessed on 27 Nov 2023]
51. Chen ZC, Wang B, Bhuckory MB, et al. Optically configurable confinement of electric field with photovoltaic retinal prosthesis. *Invest Ophthalmol Vis Sci* 2021;62:3166. Available from: <https://iovs.arvojournals.org/article.aspx?articleid=2776270>. [Last accessed on 27 Nov 2023]
52. Chenais NAL, Airaghi Leccardi MJI, Ghezzi D. Photovoltaic retinal prosthesis restores high-resolution responses to single-pixel stimulation in blind retinas. *Commun Mater* 2021;2:28. DOI
53. Loudin JD, Simanovskii DM, Vijayraghavan K, et al. Optoelectronic retinal prosthesis: system design and performance. *J Neural Eng* 2007;4:S72. DOI
54. Mathieson K, Loudin J, Goetz G, et al. Photovoltaic retinal prosthesis with high pixel density. *Nature Photon* 2012;6:391-7. DOI PubMed PMC
55. Boinagrov D, Lei X, Goetz G, et al. Photovoltaic pixels for neural stimulation: circuit models and performance. *IEEE Trans Biomed Circuits Syst* 2016;10:85-97. DOI PubMed PMC
56. Lei X, Huang TW, Flores TA, et al. Photovoltaic subretinal prosthesis with pixel sizes down to 40 um. *Invest Ophthalmol Vis Sci* 2017;58:4269. Available from: <https://iovs.arvojournals.org/article.aspx?articleid=2641379>. [Last accessed on 27 Nov 2023]
57. Bhuckory MB, Chen ZC, Shin A, et al. 3-dimensional subretinal prosthesis with single-cell resolution. *Invest Ophthalmol Vi Sci* 2022;63:4516-F0303. Available from: <https://iovs.arvojournals.org/article.aspx?articleid=2782016>. [Last accessed on 27 Nov 2023]
58. Wang BY, Chen ZC, Bhuckory M, et al. Electronic photoreceptors enable prosthetic visual acuity matching the natural resolution in rats. *Nat Commun* 2022;13:6627. DOI PubMed PMC
59. Silverå Ejneby M, Migliaccio L, Gicevičius M, et al. Extracellular photovoltage clamp using conducting polymer-modified organic



- photocapacitors. *Adv Mater Technol* 2020;5:1900860. DOI
60. Silverå Ejneby M, Jakešová M, Ferrero JJ, et al. Chronic electrical stimulation of peripheral nerves via deep-red light transduced by an implanted organic photocapacitor. *Nat Biomed Eng* 2022;6:741-53. DOI
61. Menz MD, Oralkan O, Khuri-Yakub PT, Baccus SA. Precise neural stimulation in the retina using focused ultrasound. *J Neurosci* 2013;33:4550-60. DOI PubMed PMC
62. Seo D, Neely RM, Shen K, et al. Wireless recording in the peripheral nervous system with ultrasonic neural dust. *Neuron* 2016;91:529-39. DOI
63. Marketing clearance of diagnostic ultrasound systems and transducers. Guidance for industry and food and drug administration staff. Available from: <https://www.fda.gov/media/71100/download>. [Last accessed on 27 Nov 2023].
64. Wang X, Song J, Liu J, Wang ZL. Direct-current nanogenerator driven by ultrasonic waves. *Science* 2007;316:102-5. DOI
65. Ciofani G, Danti S, D'Alessandro D, et al. Enhancement of neurite outgrowth in neuronal-like cells following boron nitride nanotube-mediated stimulation. *ACS Nano* 2010;4:6267-77. DOI
66. Marino A, Arai S, Hou Y, et al. Piezoelectric nanoparticle-assisted wireless neuronal stimulation. *ACS Nano* 2015;9:7678-89. DOI PubMed PMC
67. Piech DK, Johnson BC, Shen K, et al. A wireless millimetre-scale implantable neural stimulator with ultrasonically powered bidirectional communication. *Nat Biomed Eng* 2020;4:207-22. DOI
68. Shi Q, Wang T, Lee C. MEMS based broadband piezoelectric ultrasonic energy harvester (PUEH) for enabling self-powered implantable biomedical devices. *Sci Rep* 2016;6:24946. DOI PubMed PMC
69. Yang Z, Zeng D, Wang H, Zhao C, Tan J. Harvesting ultrasonic energy using 1-3 piezoelectric composites. *Smart Mater Struct* 2015;24:075029. DOI
70. Jiang L, Yang Y, Chen R, et al. Flexible piezoelectric ultrasonic energy harvester array for bio-implantable wireless generator. *Nano Energy* 2019;56:216-24. DOI PubMed PMC
71. Jiang L, Yang Y, Chen R, et al. Ultrasound-induced wireless energy harvesting for potential retinal electrical stimulation application. *Adv Funct Mater* 2019;29:1902522. DOI
72. Jiang L, Lu G, Zeng Y, et al. Flexible ultrasound-induced retinal stimulating piezo-arrays for biomimetic visual prostheses. *Nat Commun* 2022;13:3853. DOI PubMed PMC
73. Jiang L, Lu G, Yang Y, et al. Photoacoustic and piezo-ultrasound hybrid-induced energy transfer for 3D twining wireless multifunctional implants. *Energy Environ Sci* 2021;14:1490-505. DOI
74. Chen P, Wu P, Wan X, et al. Ultrasound-driven electrical stimulation of peripheral nerves based on implantable piezoelectric thin film nanogenerators. *Nano Energy* 2021;86:106123. DOI
75. Das R, Curry EJ, Le TT, et al. Biodegradable nanofiber bone-tissue scaffold as remotely-controlled and self-powering electrical stimulator. *Nano Energy* 2020;76:105028. DOI
76. Chen P, Wang Q, Wan X, et al. Wireless electrical stimulation of the vagus nerves by ultrasound-responsive programmable hydrogel nanogenerators for anti-inflammatory therapy in sepsis. *Nano Energy* 2021;89:106327. DOI
77. Xu Z, Wan X, Mo X, et al. Electrostatic assembly of laminated transparent piezoelectrets for epidermal and implantable electronics. *Nano Energy* 2021;89:106450. DOI
78. Wan X, Chen P, Xu Z, et al. Hybrid-piezoelectret based highly efficient ultrasonic energy harvester for implantable electronics. *Adv Funct Mater* 2022;32:2200589. DOI
79. Tofts PS. The distribution of induced currents in magnetic stimulation of the nervous system. *Phys Med Biol* 1990;35:1119-28. DOI PubMed
80. Bagherzadeh H, Meng Q, Lu H, Hong E, Yang Y, Choa FS. High-performance magnetic-core coils for targeted rodent brain stimulations. *BME Front* 2022;2022:9854846. DOI PubMed PMC
81. Klomjai W, Katz R, Lackmy-Vallée A. Basic principles of transcranial magnetic stimulation (TMS) and repetitive TMS (rTMS). *Ann Phys Rehabil Med* 2015;58:208-13. DOI PubMed
82. Deng ZD, Lisanby SH, Peterchev AV. Electric field depth-focality tradeoff in transcranial magnetic stimulation: simulation comparison of 50 coil designs. *Brain Stimul* 2013;6:1-13. DOI PubMed PMC
83. Roth Y, Amir A, Levkovitz Y, Zangen A. Three-dimensional distribution of the electric field induced in the brain by transcranial magnetic stimulation using figure-8 and deep H-coils. *J Clin Neurophysiol* 2007;24:31-8. DOI PubMed
84. Wilson SA, Day BL, Thickbroom GW, Mastaglia FL. Spatial differences in the sites of direct and indirect activation of corticospinal neurones by magnetic stimulation. *Electroencephalogr Clin Neurophysiol* 1996;101:255-61. DOI PubMed
85. Di Lazzaro V, Oliviero A, Meglio M, et al. Direct demonstration of the effect of lorazepam on the excitability of the human motor cortex. *Clin Neurophysiol* 2000;111:794-9. DOI
86. Pascual-Leone A, Valls-Solé J, Wassermann EM, Hallett M. Responses to rapid-rate transcranial magnetic stimulation of the human motor cortex. *Brain* 1994;117:847-58. DOI PubMed
87. Chen R, Classen J, Gerloff C, et al. Depression of motor cortex excitability by low-frequency transcranial magnetic stimulation. *Neurology* 1997;48:1398-403. DOI
88. Huang YZ, Edwards MJ, Rounis E, Bhatia KP, Rothwell JC. Theta burst stimulation of the human motor cortex. *Neuron* 2005;45:201-6. DOI PubMed
89. Hamada M, Hanajima R, Terao Y, et al. Quadro-pulse stimulation is more effective than paired-pulse stimulation for plasticity

- induction of the human motor cortex. *Clin Neurophysiol* 2007;118:2672-82. DOI
90. Khedr EM, Gilio F, Rothwell J. Effects of low frequency and low intensity repetitive paired pulse stimulation of the primary motor cortex. *Clin Neurophysiol* 2004;115:1259-63. DOI PubMed
  91. Park HJ, Bonmassar G, Kaltenbach JA, Machado AG, Manzoor NF, Gale JT. Activation of the central nervous system induced by micro-magnetic stimulation. *Nat Commun* 2013;4:2463. DOI PubMed PMC
  92. Khalifa A, Zaeimbashi M, Zhou TX, et al. The development of microfabricated solenoids with magnetic cores for micromagnetic neural stimulation. *Microsyst Nanoeng* 2021;7:91. DOI PubMed PMC
  93. Boyden ES, Zhang F, Bamberg E, Nagel G, Deisseroth K. Millisecond-timescale, genetically targeted optical control of neural activity. *Nat Neurosci* 2005;8:1263-8. DOI PubMed
  94. Yang Y, Wu M, Vázquez-Guardado A, et al. Wireless multilateral devices for optogenetic studies of individual and social behaviors. *Nat Neurosci* 2021;24:1035-45. DOI PubMed PMC
  95. Rajalingham R, Sorenson M, Azadi R, Bohn S, DiCarlo JJ, Afraz A. Chronically implantable LED arrays for behavioral optogenetics in primates. *Nat Methods* 2021;18:1112-6. DOI PubMed
  96. Wells J, Kao C, Mariappan K, et al. Optical stimulation of neural tissue *in vivo*. *Opt Lett* 2005;30:504-6. DOI PubMed
  97. Wu X, Jiang Y, Rommelfanger NJ, et al. Tether-free photothermal deep-brain stimulation in freely behaving mice via wide-field illumination in the near-infrared-II window. *Nat Biomed Eng* 2022;6:754-70. DOI PubMed PMC
  98. Harvey EN. The effect of high frequency sound waves on heart muscle and other irritable tissues. *Am J Physiol* 1929;91:284-90. DOI
  99. Tufail Y, Matyushov A, Baldwin N, et al. Transcranial pulsed ultrasound stimulates intact brain circuits. *Neuron* 2010;66:681-94. DOI
  100. Yoo SS, Bystritsky A, Lee JH, et al. Focused ultrasound modulates region-specific brain activity. *Neuroimage* 2011;56:1267-75. DOI PubMed PMC
  101. Lee W, Lee SD, Park MY, et al. Image-guided focused ultrasound-mediated regional brain stimulation in sheep. *Ultrasound Med Biol* 2016;42:459-70. DOI
  102. Dallapiazza RF, Timbie KF, Holmberg S, et al. Noninvasive neuromodulation and thalamic mapping with low-intensity focused ultrasound. *J Neurosurg* 2018;128:875-84. DOI PubMed PMC
  103. Deffieux T, Younan Y, Wattiez N, Tanter M, Pouget P, Aubry JF. Low-intensity focused ultrasound modulates monkey visuomotor behavior. *Curr Biol* 2013;23:2430-3. DOI PubMed
  104. Legon W, Bansal P, Tyshynsky R, Ai L, Mueller JK. Transcranial focused ultrasound neuromodulation of the human primary motor cortex. *Sci Rep* 2018;8:10007. DOI PubMed PMC
  105. Panczykowski DM, Monaco EA III, Friedlander RM. Transcranial focused ultrasound modulates the activity of primary somatosensory cortex in humans. *Neurosurgery* 2014;74:N8-9. DOI PubMed
  106. Zhang F, Aravanis AM, Adamantidis A, de Lecea L, Deisseroth K. Circuit-breakers: optical technologies for probing neural signals and systems. *Nat Rev Neurosci* 2007;8:577-81. DOI PubMed
  107. Wagner T, Valero-Cabre A, Pascual-Leone A. Noninvasive human brain stimulation. *Annu Rev Biomed Eng* 2007;9:527-65. DOI PubMed
  108. Dalecki D. Mechanical bioeffects of ultrasound. *Annu Rev Biomed Eng* 2004;6:229-48. DOI PubMed
  109. Dinno MA, Dyson M, Young SR, Mortimer AJ, Hart J, Crum LA. The significance of membrane changes in the safe and effective use of therapeutic and diagnostic ultrasound. *Phys Med Biol* 1989;34:1543-52. DOI PubMed
  110. Ye J, Tang S, Meng L, et al. Ultrasonic control of neural activity through activation of the mechanosensitive channel MscL. *Nano Lett* 2018;18:4148-55. DOI
  111. Li J, Ma Y, Zhang T, Shung KK, Zhu B. Recent advancements in ultrasound transducer: from material strategies to biomedical applications. *BME Front* 2022;2022:9764501. DOI PubMed PMC
  112. Qian X, Lu G, Thomas BB, et al. Noninvasive ultrasound retinal stimulation for vision restoration at high spatiotemporal resolution. *BME Front* 2022;2022:9829316. DOI PubMed PMC
  113. Zhang T, Wang Z, Liang H, et al. Transcranial focused ultrasound stimulation of periaqueductal gray for analgesia. *IEEE Trans Biomed Eng* 2022;69:3155-62. DOI
  114. Kook G, Jo Y, Oh C, et al. Multifocal skull-compensated transcranial focused ultrasound system for neuromodulation applications based on acoustic holography. *Microsyst Nanoeng* 2023;9:45. DOI PubMed PMC
  115. Jiang Y, Lee HJ, Lan L, et al. Optoacoustic brain stimulation at submillimeter spatial precision. *Nat Commun* 2020;11:881. DOI PubMed PMC
  116. Shi L, Jiang Y, Fernandez FR, et al. Non-genetic photoacoustic stimulation of single neurons by a tapered fiber optoacoustic emitter. *Light Sci Appl* 2021;10:143. DOI PubMed PMC
  117. Zheng N, Fitzpatrick V, Cheng R, Shi L, Kaplan DL, Yang C. Photoacoustic carbon nanotubes embedded silk scaffolds for neural stimulation and regeneration. *ACS Nano* 2022;16:2292-305. DOI PubMed